

## Article

# Thinning vs. Pruning: Impacts on Sap Flow Density and Water Use Efficiency in Young *Populus tomentosa* Plantations in Northern China

Yan Liu <sup>1,2,3</sup>, Yadong Liu <sup>1,2,3</sup>, Shuanglei Qi <sup>1,2</sup>, Ziyang Fan <sup>1,2</sup>, Yadan Xue <sup>1,2</sup>, Qingxuan Tang <sup>1,2</sup>, Zhengyuan Liu <sup>1,2</sup>, Xiaomin Zheng <sup>1,2,3</sup>, Chuangye Wu <sup>4</sup>, Benye Xi <sup>1,2</sup>  and Jie Duan <sup>1,2,3,\*</sup> 

- <sup>1</sup> State Key Laboratory of Efficient Production of Forest Resources, Beijing Forestry University, Beijing 100083, China; dooby@bjfu.edu.cn (Y.L.); liuyadong@bjfu.edu.cn (Y.L.); qishuanglei1@bjfu.edu.cn (S.Q.); fanziying22@bjfu.edu.cn (Z.F.); xueyadan1@bjfu.edu.cn (Y.X.); tangqingxuan24@bjfu.edu.cn (Q.T.); liuzhengyuan@bjfu.edu.cn (Z.L.); zhengxiaomin@bjfu.edu.cn (X.Z.); benyexi@bjfu.edu.cn (B.X.)
- <sup>2</sup> Key Laboratory for Silviculture and Forest Ecosystem in Arid- and Semi-Arid Region of State Forestry and Grassland Administration, Beijing 100083, China
- <sup>3</sup> National Energy R&D Center for Non-Food Biomass (NECB), Beijing Forestry University, Beijing 100083, China
- <sup>4</sup> Wen County Forestry Science Research Institution, Jiaozuo 454850, China; wxmp12@163.com
- \* Correspondence: duanjie@bjfu.edu.cn; Tel.: +86-10-6233-6536

**Abstract:** Water is a vital resource for tree growth, and changes in plantation and canopy structure can affect stand transpiration ( $E_c$ ), consequently influencing water use efficiency ( $WUE$ ). *Populus tomentosa* is a fast-growing and productive timber species in China. In recent years, thinning combined with pruning has become a widely used silvicultural practice for timber management. However, its effect on water utilization has been less well studied. To address this gap, we designed experiments with two thinning intensities and three pruning treatments. Thermal dissipation probes were employed to monitor tree sap flow density ( $J_s$ ), and estimated  $E_c$  and canopy conductance ( $g_c$ ). We established a relationship between the canopy transpiration per unit leaf area ( $E_L$ ) and  $g_c$  and climatic factors. Finally, we compared basal area increment ( $BAI$ ) and  $WUE$  among treatments under different rainfall conditions. The results indicated that: (1) The pattern of transpiration changes was consistent at both the individual tree and stand level. (2) The combined effect of T1 (thinning intensity of 833 trees per hectare) and pruning reduced  $E_c$ , decreasing the sensitivity of tree transpiration to the climate, with no discernible impact on  $E_L$  and  $g_c$ . Conversely, T2 (thinning intensity of 416 trees per hectare) and pruning increased  $E_L$  and  $g_c$  but had no effect on  $E_c$ , enhancing the sensitivity of tree transpiration to the climate. The sensitivity of  $g_c$  to  $VPD$  suggested a flexible stomatal regulation of transpiration under different combined thinning and pruning treatments. (3) Under T1, only P2 (4 m pruning from ground) promoted  $WUE$ , while pruning effects significantly reduced  $WUE$  under T2. Overall, the  $WUE$  of T2P0 (thinning intensity of 416 trees per hectare combined with no pruning) was significantly higher than that of the other treatments, and that of T1P0 (thinning intensity of 833 trees per hectare combined with no pruning) was significantly lower than that of the other treatments. Additionally, significant differences in  $E_c$  and  $BAI$  were observed among treatments under different rainfall conditions, with the promotion effect of  $E_c$  on  $BAI$  being more pronounced in the dry season.

**Keywords:** thinning; pruning; sap flow density; water use efficiency; *Populus tomentosa*



**Citation:** Liu, Y.; Liu, Y.; Qi, S.; Fan, Z.; Xue, Y.; Tang, Q.; Liu, Z.; Zheng, X.; Wu, C.; Xi, B.; et al. Thinning vs. Pruning: Impacts on Sap Flow Density and Water Use Efficiency in Young *Populus tomentosa* Plantations in Northern China. *Forests* **2024**, *15*, 536. <https://doi.org/10.3390/f15030536>

Academic Editor: Luca Belelli Marchesini

Received: 5 February 2024

Revised: 4 March 2024

Accepted: 12 March 2024

Published: 14 March 2024



**Copyright:** © 2024 by the authors. Licensee MDPI, Basel, Switzerland. This article is an open access article distributed under the terms and conditions of the Creative Commons Attribution (CC BY) license (<https://creativecommons.org/licenses/by/4.0/>).

## 1. Introduction

Plantations are the largest terrestrial ecosystems, covering more than 30% of global land. Plantations are crucial in maintaining biodiversity, regulating climate, conserving water resources, and providing numerous ecological services, production, and other industries [1]. Plantations are a viable solution for meeting timber demand, and they currently cover about 3% (about 1.31 billion ha) of the global forest area, with China leading

the world in planted forest area at about 0.89 billion ha [1–4]. However, in contrast to natural forests, plantations are more vulnerable to environmental changes, such as rising temperatures and decreasing water availability, which may impede their growth in the future [5–8]. Conventional plantation management practices are designed to promote growth by regulating the resources available to the trees and increasing their efficiency. Thinning alters the access of individual trees to resources like light, water, and nutrients, while pruning is an important management practice to produce high-quality, knot-free timber with large diameters by removing the shaded and least-efficient foliage, regulating the distribution of photosynthates among organs, and increasing aboveground biomass allocation utilization efficiency [9–13]. However, there is limited research on how these management practices affect the physiological and ecological processes that respond to the environment of plantations.

Thinning and pruning represent common practices in sustainable plantation management. Thinning can enhance tree growth and increase radial growth [14–16]. However, some studies have found that thinning in arid regions does not significantly affect radial growth [17]. Additionally, thinning can reduce the vulnerability of plantations to climate change, such as drought [18,19], improve *WUE* [18,20], and mitigate drought-induced growth decline [21,22]. Pruning lower-level canopy branches and leaves can increase knot-free timber yield [19,23] and may not influence growth, as decreases in canopy resource capture rates are often offset by increases in the photosynthetic efficiency of the remaining canopy leaves [11,24–26]. The effects of thinning and pruning on tree growth are not uniform, and few studies have reported on the combined effects. Forrester et al. [9,11,27] studied the effects of coupled thinning and pruning on Eucalyptus growth and found that thinning had a more significant impact on growth than pruning.

Water is a vital resource for tree growth, and tree transpiration plays a crucial role in the water cycle of terrestrial ecosystems [28]. Plantation management can affect tree–water physiological and ecological processes. Thinning can reduce stand density and directly alter photosynthetically active radiation (*PAR*) and vapor pressure deficit (*VPD*) [29–31], thereby affecting tree transpiration and canopy conductance [32–34]. Previous research has demonstrated that thinning can lead to an increase in tree sap flow density [15,21], significantly enhancing tree transpiration [18,35]. The widely adopted sap flow density method is particularly effective for assessing transpiration from individual trees and can be extrapolated to the stand level [36,37]. It is crucial to note that the response of stands to water conditions differs significantly from that of individual trees [38]. After thinning, a reduction in tree amount reduces stand-level transpiration [21,39]. However, some studies have shown that stand transpiration after thinning was significantly different from that before thinning [40]. This outcome is attributed to factors such as increased photosynthetically active radiation, improved air movement within the canopy, and enhanced water and nutrient availability for retained individual trees, all contributing to heightened transpiration [41,42]. Meanwhile the majority of studies indicate that pruning significantly reduces tree transpiration [35,43], though this effect may only be observed in the short term [23].

*WUE* represents the carbon gain efficiency per water consumption unit [44,45]. At both the individual tree and stand levels, *WUE* is often determined by using the ratio of diameter increments at breast height (*DBH*) to transpiration [46]. Plantation management practices such as thinning and pruning can increase *WUE* by providing more light to the lower canopy and improving the efficiency of the remaining foliage [11,15,16,21,47,48]. Understanding *WUE* under the combined effects of thinning and pruning is crucial to comprehend and regulate the forest water cycle, as well as to optimize plantation management practices.

Poplar (*Populus* spp.) is a fast-growing and adaptable tree widely recognized as a vital species in timber production and ecological services. The area of poplar plantations in China has reached 8.5 million hectares, accounting for 27% of the total plantation area in the country, making it the largest area of poplar plantations in the world [30]. *Populus tomentosa* is the predominant species in poplar plantations across the North China

Plain region and is the first development species in the National Reserve Forest Program from 2018 to 2035 [4]. In recent years, thinning combined with pruning has become a widely used plantation management practice that enhances wood yield and quality [49]. Although the growth-promoting effects of combined thinning and pruning have been demonstrated in species such as Eucalyptus (*Eucalyptus nitens*) [11], Pine (*Pinus patula*) [50], Sitka spruce (*Picea sitchensis*), Western hemlock (*Tsuga heterophylla*) [49], and European beech (*Fagus sylvatica* L.) [51], no research has yet been conducted on the effects of this combination of treatments on sap flow density and *WUE* specifically in poplar.

The primary objective of this study was to examine the combined effects of two thinning intensities and three pruning heights on the transpiration of 4-year-old *Populus tomentosa* at the stand and individual levels during the growing season of June–October 2022. Furthermore, the regulation mechanism of tree–water relations under different treatments was explored through the sensitivity of  $g_c$  to *VPD*, and the relationship between *WUE* and the growth of trees in different rainfall periods under diverse treatments was also investigated. The specific scientific questions addressed were: (1) Is there a consistent response pattern of transpiration in single trees and stands under different combinations of thinning and pruning? (2) Are there differences in stand-level  $g_c$  and transpiration and their relationships with environmental factors under the different thinning and pruning combinations? (3) Are there differences in stand *WUE* among the different thinning and pruning combinations? The result of this study can provide helpful information to inform the basis for poplar plantation management strategies to mitigate tree stress under changing environmental conditions.

## 2. Materials and Methods

### 2.1. Introduction to Study Sites and Species

The experiment was conducted at the Wen County Forestry Science Research Institution, situated in Henan Province (34°50′~35°03′ N, 112°51′~113°13′ E), with an elevation of 102.3~116.1 m (Figure 1). This area has a warm temperate continental monsoon climate, featuring an average annual temperature of 14.3 °C, and an average annual precipitation of 552.4 mm, of which 80% precipitation is during the rainy season from June to September.

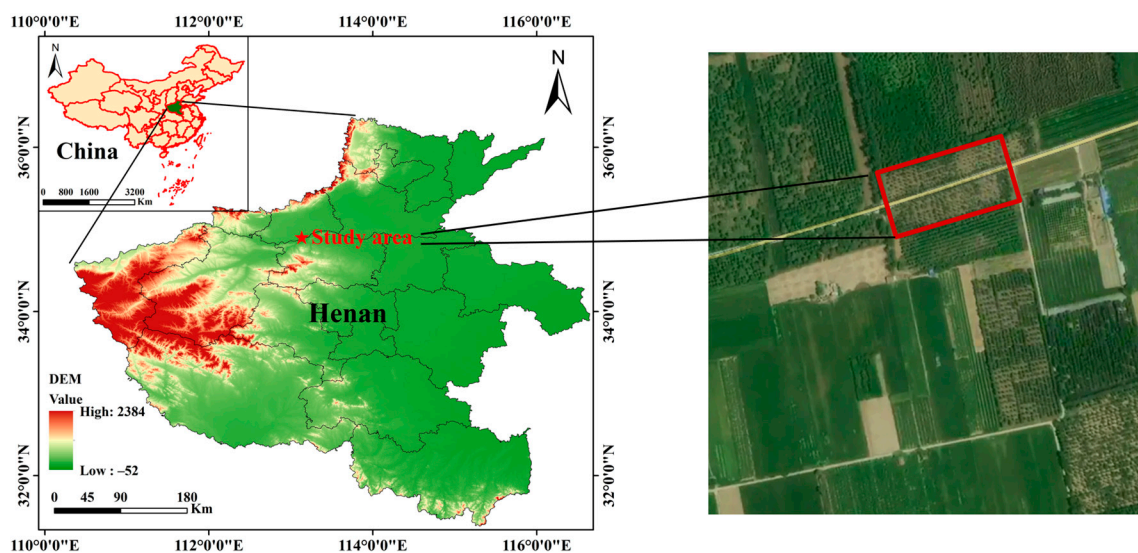


**Figure 1.** Location of the study site.

In 2018, the experimental plantation of *P. tomentosa* ‘Jiangan No.1’ was established at a density of 1666 trees ha<sup>-1</sup> (1.5 m × 4 m). In the spring of 2022, a randomized block design was employed in a 2 × 3 factorial scheme with two thinning intensities (833 trees per hectare, T1, and 416 trees per hectare, T2) and three pruning heights (no pruning, P0; 3 m pruning from ground, P1; and 4 m pruning from ground, P2) across three 60 × 40 m

blocks (blocks I, II, and III). Six combined treatments were implemented: 3 × 4 m—no pruning (T1P0), 3 × 4 m—3 m pruning (T1P1), 3 × 4 m—4 m pruning (T1P2), 6 × 4 m—no pruning (T2P0), 6 × 4 m—3 m pruning (T2P1), 6 × 4 m—4 m pruning (T2P2) (Figure 2). Each treatment had three replicates, each with a randomized plot measuring 20 m × 20 m, resulting in 18 plots.

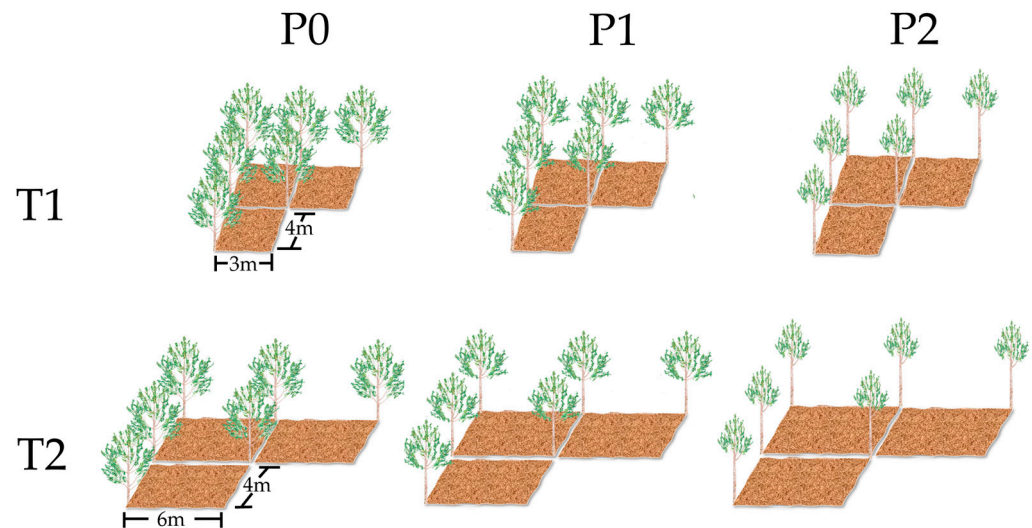


**Figure 2.** Schematic diagram of experimental design.

An automatic weather station (Sinton Technology Ltd., Beijing, China) was installed at a distance of 200 m from the experimental site to continuously monitor meteorological variables such as wind speed ( $W_s$ ,  $\text{m s}^{-1}$ ), photosynthetically active radiation ( $PAR$ ,  $\mu\text{mol m}^{-2} \text{s}^{-1}$ ), air temperature ( $T_{\text{air}}$ ,  $^{\circ}\text{C}$ ), and relative air humidity ( $RH$ , %) at 2 m, precipitation ( $P$ , mm), soil volumetric water content ( $\theta$ ,  $\text{m}^3 \text{m}^{-3}$ ), and soil temperature ( $T_{\text{soil}}$ ,  $^{\circ}\text{C}$ ). Meteorological data were recorded at 10 min intervals. The atmospheric vapor pressure deficit ( $VPD$ , kPa) was calculated according to the empirical equation developed by Campbell and Norman (1998) [52], while reference evapotranspiration ( $ET_0$ ,  $\text{mm d}^{-1}$ ) was calculated by the Penman–Monteith equation as recommended by FAO-56 (Allen et al., 1998 [53]):

$$ET_0 = \frac{0.408\Delta(R_n - G) + \gamma \frac{900}{T_{\text{air}} + 273} W_s (e_s - e_a)}{\Delta + \gamma(1 + 0.34)W_s} \quad (1)$$

where  $R_n$  is the net radiation ( $\text{MJ m}^{-2} \text{d}^{-1}$ );  $G$  is the soil heat flux density ( $\text{MJ m}^{-2} \text{d}^{-1}$ ) (soil heat flux beneath the vegetation is relatively small for the daily average, it may be neglected, i.e.,  $G \approx 0$ );  $T_{\text{air}}$  is the mean air temperature ( $^{\circ}\text{C}$ );  $W_s$  is the wind speed at 2 m height above ground ( $\text{m s}^{-1}$ ),  $e_s$  is saturation vapor pressure (kPa),  $e_a$  is actual vapor pressure (kPa);  $\Delta$  is the slope of the relationship curve between saturation vapor pressure and temperature ( $\text{kPa } ^{\circ}\text{C}^{-1}$ ); and  $\gamma$  is the psychrometric constant ( $\text{kPa } ^{\circ}\text{C}^{-1}$ ).

Leaf area index ( $LAI$ ,  $\text{m}^2 \text{m}^{-2}$ ) was measured every two weeks by using a Yaxin-1201 plant canopy analyzer (Yasin Science and Technology Ltd., Beijing, China) from June to November 2022. We selected 5 positions in each treatment, and then obtained the  $LAI$  values through the software. Their mean values were calculated as the representative  $LAI$  for each treatment. Finally, we fitted the time dynamics of the mean values of  $LAI$  for each treatment by using linear interpolation (Figure S1).

## 2.2. Sap Flow Density Measurement and Stand Transpiration Estimation

### 2.2.1. Sampling Tree Selection

According to the frequency distribution of  $DBH$  from three replicated blocks (surveyed before sap flow density measurement), three sample trees were selected for each treatment



plot. The variations in *DBH* of the selected three sampling trees for sap flow density measurement mainly ranged between 7 cm and 9 cm, following the interval probabilities for normal distribution and reflecting the average stand growth status (Table 1; Figure S2).

**Table 1.** Traits of the sampling trees in T1P0, T1P1, T1P2, T2P0, T2P1, T2P2.

Treatment	Tree Number	Height (m)	<i>DBH</i> (cm)	Height to Canopy Base (m)	Crown Width (m)	SA (cm <sup>2</sup> )
T1P0	1	7.6	8.18	2.7	2.7 × 3.6	46.10
	2	8.8	7.9	2.4	2.8 × 3.6	43.06
	3	10.2	8.21	2	3.3 × 3.8	46.43
T1P1	4	7.7	8.5	2.4	2.3 × 3.6	49.69
	5	8.8	8.12	2.6	2.7 × 2.9	45.44
	6	7.2	7.22	2.3	2.2 × 2.1	36.12
T1P2	7	8	8.76	2.18	2.2 × 3.7	52.70
	8	8.1	8.52	2.6	2.8 × 3.7	49.92
	9	7.8	6.82	2.1	3 × 3	32.31
T2P0	10	9.3	9	2.2	3.1 × 3.9	55.56
	11	10.3	9.22	2.4	3.4 × 4.5	58.24
	12	7.3	7.7	2.3	2.2 × 2.8	40.96
T2P1	13	9.4	8.31	2.7	2.8 × 4	47.54
	14	8.4	7.75	2.07	2.3 × 3.3	41.48
	15	8.5	8.38	2.1	2.3 × 3.1	48.33
T2P2	16	7.5	7.85	2.2	3 × 3.2	42.53
	17	8.6	7.35	2.3	2.5 × 2.9	37.40
	18	8.8	7.7	2.3	3.4 × 4.6	40.96

### 2.2.2. Probe Installation and Calculation of Sap Flow Density

Sap flow density ( $J_s$ , cm s<sup>-1</sup>) was obtained by the thermal dissipation probes (TD-30, 3 cm in length) (Dynamax Inc., Houston, TX, USA). The probes were inserted into the sapwood on the north-facing side of each sampling tree at a height of 1.3 m–1.5 m above the ground. To prevent exposure to precipitation and thermal radiation effects, the probes were cemented with waterproof glue, and we used foam to fix them. At last, reflective bubble insulation was wrapped around the probes and the stem [28]. The  $J_s$  was measured every 10 s, and its average value, calculated every 10 min, was stored in the data loggers (CR1000, Campbell Scientific Inc., Logan, UT, USA).  $J_s$  was estimated using the formula proposed by Granier (1987) [54]:

$$J_s = 0.0119 \times K^{1.231} \quad (2)$$

where the temperature difference coefficient  $K = (dT_M - dT)/dT$ ;  $dT_M$  is the maximal temperature difference between two probes (°C);  $dT$  is the temperature difference between the heated probe and unheated reference probe (°C);  $dT_M$  is determined over a 7–10-day period by taking the maximum value of  $dT$  to avoid the underestimation of night-time  $J_s$ .

The  $J_s$  measured using the TD-30 probes can be influenced by many error sources, such as wounding, radial velocity profile, and wood properties [55–57]. It has been found in many studies that  $J_s$  can be over- or under-estimated to different degrees [56,58,59]. Therefore, we have verified that the original Granier's equation of Equation (2) is credible as accurate and valid for our *P. tomentosa* plantation [60,61], and the variation in azimuthal was ignored. And this function has been also widely applied to many related studies on poplars [30,62,63].

### 2.2.3. Estimation of Transpiration and Canopy Conductance

The whole-tree transpiration ( $E_t$ , mm d<sup>-1</sup>) was calculated according to the following equation [64]:

$$E_t = J_s \left( \frac{A_{s-plot}}{A_{g-plot}} \right) \quad (3)$$

where  $J_s$  is the standard wood sap flow density (cm s<sup>-1</sup>);  $A_{s-plot}$  is the sampling tree sapwood area (cm<sup>2</sup>); and  $A_{g-plot}$  is the plot area per sampling tree (cm<sup>2</sup>) (the  $A_{g-plot}$  at T1 and T2 are 12 m<sup>2</sup> and 24 m<sup>2</sup>, respectively).

Due to the high variability in  $J_s$  in single trees, the sapwood area-weighted average fluid flow density ( $J_m$ ) of all sampling trees was employed to extend from single trees to the stand scale. Subsequently, daily scale transpiration ( $E_c$ , mm d<sup>-1</sup>) was derived by multiplying  $J_m$  and the sapwood area index (SAI) (sapwood area per stand ground surface) [65].

$$E_c = J_m \frac{A_{s-stand}}{A_{g-stand}} \quad (4)$$

where  $A_{s-stand}$  is the total sapwood area of the stand (cm<sup>2</sup>), and  $A_{g-stand}$  is the total ground area of the stand (m<sup>2</sup>) (1200 m<sup>2</sup>).

The sapwood area ( $A_s$ ) was calculated by using the anisotropic equation established in the previous study on *P. tomentosa* by Zhao et al. (2023) [36], with the diameter at the location of the  $J_s$  measurement as the independent variable ( $A_s = 0.7587 \times DBH^{1.9541}$ ). Additionally, the canopy transpiration per unit leaf area ( $E_L$ , mm d<sup>-1</sup>) was estimated by dividing  $E_c$  by the leaf area index (LAI, m<sup>2</sup> m<sup>-2</sup>) [66]. Canopy conductance ( $g_c$ , mm s<sup>-1</sup>) was calculated from  $E_L$  through a simplified reverse form of the Penman–Monteith equation [67]:

$$g_c = \frac{\gamma \lambda E_L G_a}{\Delta R_n + \rho C_p VPD G_a - \lambda (\Delta + \gamma) E_L} \quad (5)$$

where  $\Delta$  (kPa °C<sup>-1</sup>) is the slope of the saturation vapor pressure curve at  $T_{air}$ ;  $R_n$  (MJ m<sup>-2</sup>) is the net radiation;  $\gamma$  (kPa °C<sup>-1</sup>) is the psychrometric constant;  $\lambda$  (MJ kg<sup>-1</sup>) is the latent heat of vaporization of water;  $G_a$  (m s<sup>-1</sup>) is aerodynamic conductance;  $\rho$  (kg m<sup>-3</sup>) is the density of the air; and  $C_p$  (MJ kg<sup>-1</sup> °C<sup>-1</sup>) is the specific heat of air at constant pressure.

Aerodynamic conductance was calculated from wind speed using the following equation [68]:

$$G_a = \frac{k^2 \cdot u_z}{\left[ \ln \left( \frac{z-d}{z_o} \right) \right]^2} \quad (6)$$

where  $u_z$  (m s<sup>-1</sup>) is the wind speed above the forest canopy;  $z$  (m) is the wind measurement height;  $z_o$  is the roughness height (0.1 h);  $d$  is the displacement height (0.75 h);  $h$  is the forest canopy height; and  $k$  (0.4) is the von Karman constant.  $u_z$  was calculated from the measured wind speed at 2.0 m height ( $u_2$ ) based on Equation (7) [53]:

$$u_z = \frac{\ln(67.8z - 5.42)}{4.87} u_2 \quad (7)$$

### 2.2.4. The Sensitivity of Canopy Conductance to VPD

The sensitivity of  $g_c$  to VPD was calculated as follows [69]:

$$g_c = -m \ln VPD + g_{cr} \quad (8)$$

where  $-m$  represents the sensitivity of  $g_c$  to VPD.  $g_{cr}$  is reference canopy conductance when VPD is 1.0 kPa and can be used as a surrogate for the maximum  $g_c$  [70]. The ratio of  $m/g_{cr}$  can be used as a criterion for evaluating the response of tree species to environmental conditions, and despite the different environmental conditions under which they are grown,

most species have  $m/g_{cr}$  ratios of  $\sim 0.6$ , with values less than 0.6 indicating that leaf water potential is not tightly regulated and values greater than 0.6 indicating that the ratio of boundary layer conductance to canopy conductance is low in the leaf [69,71].

### 2.2.5. Stand-Level Water Use Efficiency

Stand-scale water use efficiency was calculated as follows [19]:

$$WUE = \frac{BAI}{E_c} \quad (9)$$

where  $BAI$  and  $E_c$  are the total basal area increment and transpiration, respectively. Monthly  $BAI$  was obtained from the difference in basal area ( $BA$ ) at the stand scale between two adjacent months, and  $BAI$  for the main growing season (June–October) was obtained from the difference between the  $BA$  in October and the  $BA$  in June. We calculated  $BA$  through  $DBH$ , which was measured at the beginning of each month.

### 2.3. Statistical Analysis

Data analysis in this study was conducted from 18 June to 25 October. The data collected from the thermal dissipation probes were processed and calculated by using Baseline software (version 3.0, Ram Oren, Duke University, Durham, NC, USA) [72]. Two-way analysis of variance (ANOVA) was performed on  $E_t$ ,  $J_s$ ,  $E_c$ ,  $E_L$ , and  $g_s$  to explore the interaction effects of different treatments on each indicator. Tukey's mean comparison test was then applied at a 5% significance level using the statistical software SPSS 22.0 (IBM Corporation, Chicago, IL, USA). Standardized major axis (SMA) regression analysis was used to test the differences between the slopes of the equation of different meteorological factors with  $E_L$ .

To ensure accurate estimations of  $g_c$ , only data corresponding to  $VPD$  greater than 0.6 kPa and  $PAR$  greater than  $100 \mu\text{mol m}^{-2} \text{s}^{-1}$  were selected. Boundary line analysis (BLA) was employed to analyze the physiological reactions of  $g_c$  and  $VPD$  under the given conditions [73] (Figure S3). All  $g_c$  data were sorted into intervals of  $VPD = 0.2$  kPa. The means and standard deviations of  $g_c$  were calculated based on the  $VPD$  intervals, and outliers were excluded according to the Dixon test ( $p < 0.05$ ). Intervals with  $n < 5$  were excluded to avoid the influence of inadequate information about the  $VPD$  interval on the relationship [73]. Values of  $g_c$  above the mean and one standard deviation from each  $VPD$  interval were filtered for fitting. The figures were drawn using Origin 2022b (OriginLab Corporation, Northampton, MA, USA).

## 3. Results

### 3.1. Environmental Variables and Soil Moisture

The daily mean  $T_{air}$  during the study period showed a decreasing trend, with the highest value recorded in June and values ranging from  $8.1^\circ\text{C}$  to  $33.14^\circ\text{C}$  (Figure 3a). Similarly, the daily mean  $RH$  increased and then decreased, reaching its peak in July with a range of 38.38% to 96.85% (Figure 3a). The daily mean  $PAR$  and  $VPD$  both had their highest values in June, before declining, with ranges of  $22.24 \mu\text{mol m}^{-2} \text{s}^{-1}$  to  $475.95 \mu\text{mol m}^{-2} \text{s}^{-1}$  and  $0.09$  kPa to  $3.14$  kPa, respectively (Figure 3b). The daily mean  $W_s$  had a maximum of  $1.73 \text{ m s}^{-1}$  during the measurement period (Figure 3c). Rainfall  $P$  was unevenly distributed, with a total of  $313.69$  mm accumulated (Figure 3c). The daily mean  $\theta$  increased with rainfall and decreased afterwards, varying from  $13.66 \text{ m}^3 \text{ m}^{-3}$  to  $17.79 \text{ m}^3 \text{ m}^{-3}$  (Figure 3d). The daily mean  $ET_0$  generally decreased, fluctuating between  $0.72$  mm and  $6.84$  mm (Figure 3d).

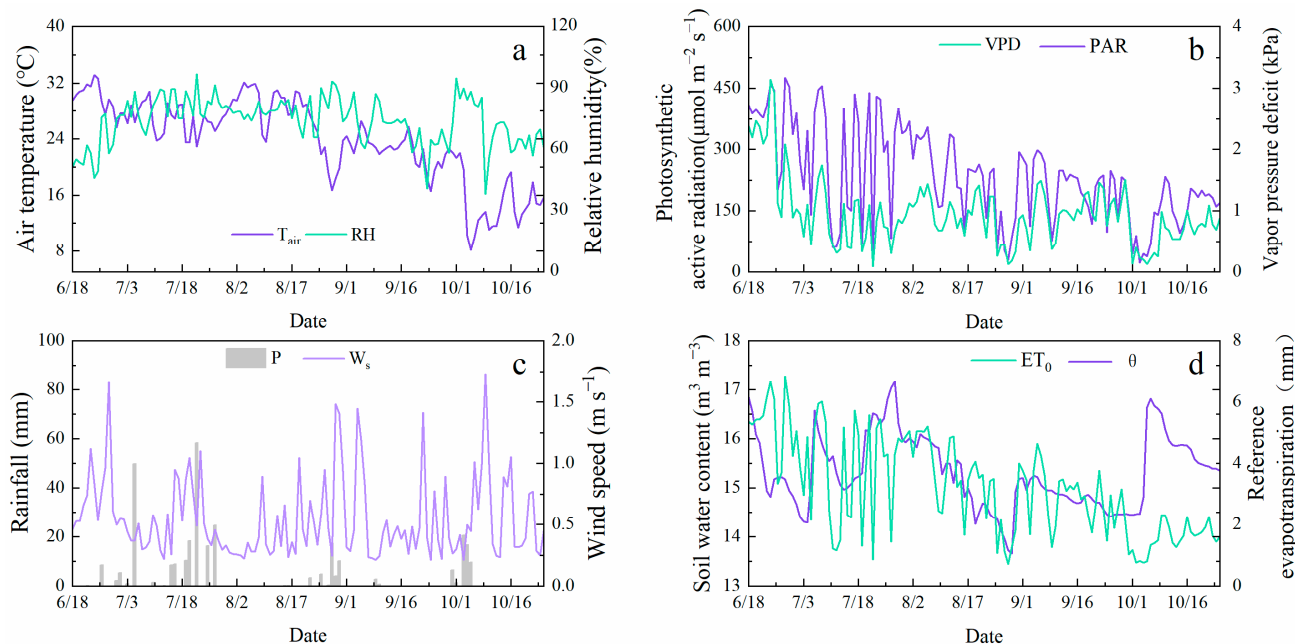


**Figure 3.** Seasonal variations in daily mean values of air temperature ((a),  $T_{air}$ ), relative humidity ((a),  $RH$ ), photosynthetic active radiation ((b),  $PAR$ ), vapor pressure deficit ((b),  $VPD$ ), daily total rainfall ((c),  $P$ ), wind speed at 2 m height ((c),  $W_s$ ), soil water content ((d),  $\theta$ ) at the depths of 20 cm soil layer, and reference evapotranspiration ((d),  $ET_0$ ) in 2022 main growing season.

### 3.2. Dynamics of Sap Flow Density, Individual Tree and Stand-Level Transpiration, and Canopy Conductance

#### 3.2.1. Sap Flow Density

The daily variations in  $J_m$  exhibited similar dynamic patterns across all treatments, displaying a continuous response to environmental conditions similar to the daily changes in  $T_{air}$ ,  $PAR$ , and  $VPD$ . It tended to increase, reaching a peak around 4:00 a.m., as  $T_{air}$ ,  $PAR$ , and  $VPD$  increased. Subsequently,  $J_m$  gradually declined after maintaining a relatively higher level between 8:00 a.m. and 4:00 p.m., approaching zero during the nighttime (Figure 4).

The interaction effect of  $J_m$  was significant (Table 2). In T1, the  $J_m$  significantly decreased by 16.81% in P2 compared to P0 ( $p < 0.001$ ), while there were no significant differences in  $J_m$  between P1 and P2 ( $p > 0.05$ ). Similarly, the  $J_m$  significantly increased by 41.08% in P2 compared to P0 for the same T2 treatment ( $p < 0.001$ ), while there were no significant differences in  $J_m$  between P1 and P0 ( $p > 0.05$ ) (Table 3). Regardless of any pruning treatments, the  $J_m$  reduced by 42.83% for T2P0 relative to T1P0, 27.71% for T2P1 relative to T1P1, and 3.05% for T2P2 relative to T1P2 due to thinning (Table 3).

**Table 2.** Two-way analysis of variance (ANOVA) of transpiration ( $E_t$ ), sapwood area-weighted mean sap flow density ( $J_m$ ), stand transpiration ( $E_c$ ), transpiration per unit leaf area ( $E_L$ ), and canopy conductance ( $g_c$ ) of different treatments.

Variables	Thinning		Pruning		Thinning × Pruning	
	F	p	F	p	F	p
$E_t$	788.026	<0.001	7.786	<0.001	9.737	<0.001
$J_m$	101.589	<0.001	1.746	0.175	25.299	<0.001
$E_c$	222.487	<0.001	4.836	<0.05	17.827	<0.001
$E_L$	3.236	0.072	13.777	<0.001	13.690	<0.001
$g_c$	10.288	0.001	14.455	<0.001	19.776	<0.001



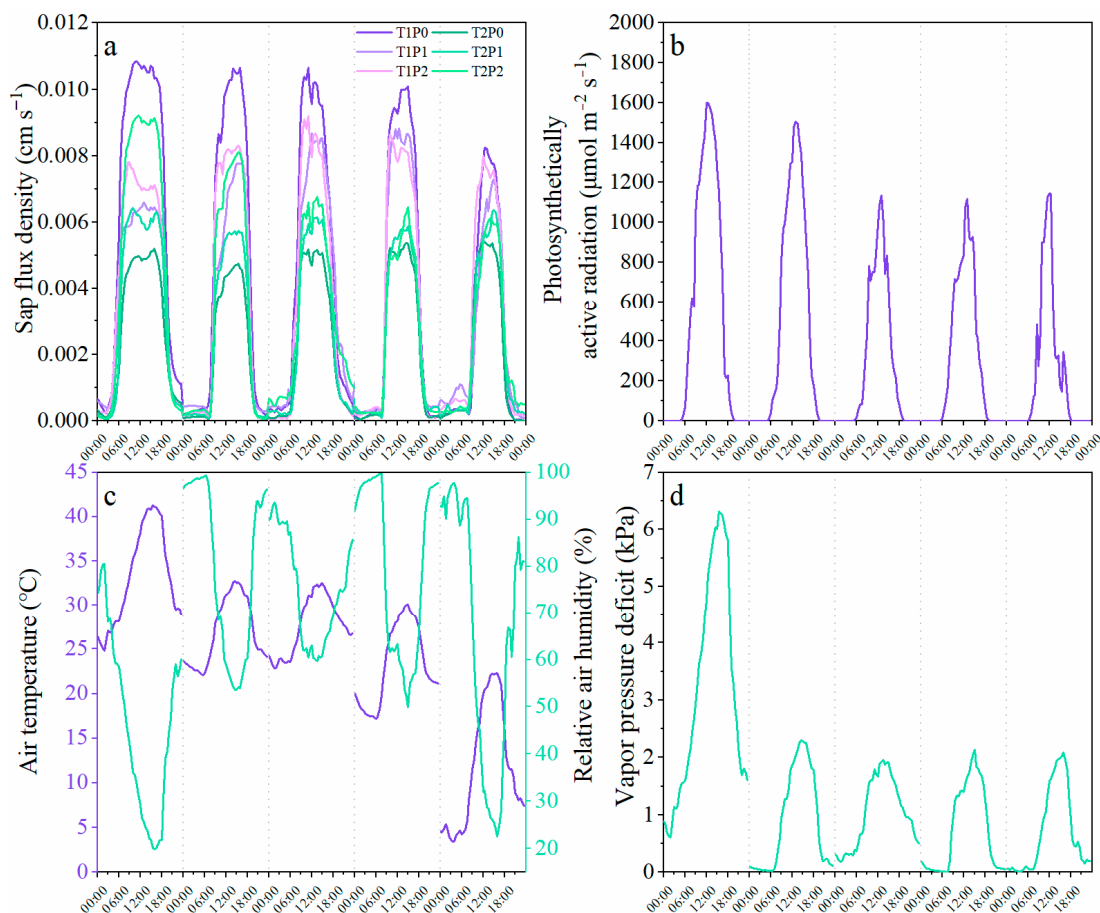


**Figure 4.** Diurnal course of sap flow density ( $J_m$ ) of different treatments (a) for five selected sunny days (24 June, 29 July, 17 August, 2 September, and 11 October) and the corresponding daily photosynthetically active radiation (PAR) (b), air temperature ( $T_{air}$ ), relative air humidity (RH) (c), and vapor pressure deficit (VPD) (d).

**Table 3.** Mean ( $\pm$ standard deviation) values of individual transpiration ( $E_t$ ), sapwood area-weighted mean sap flow density ( $J_m$ ), stand transpiration ( $E_c$ ), transpiration per unit leaf area ( $E_L$ ), and canopy conductance ( $g_c$ ) of different treatments.

Variables	T1P0	T1P1	T1P2	T2P0	T2P1	T2P2
$E_t$ (mm d <sup>-1</sup> )	1.5 $\pm$ 0.66 a	1.27 $\pm$ 0.49 b	1.24 $\pm$ 0.45 b	0.51 $\pm$ 0.18 c	0.47 $\pm$ 0.17 c	0.57 $\pm$ 0.21 c
$J_m$ (cm s <sup>-1</sup> )	0.0032 $\pm$ 0.0015 a	0.0029 $\pm$ 0.0011 ab	0.0027 $\pm$ 0.0010 b	0.0018 $\pm$ 0.0007 c	0.0021 $\pm$ 0.0008 c	0.0026 $\pm$ 0.0010 b
$E_c$ (mm d <sup>-1</sup> )	0.83 $\pm$ 0.37 a	0.69 $\pm$ 0.26 b	0.65 $\pm$ 0.24 b	0.43 $\pm$ 0.15 c	0.47 $\pm$ 0.17 c	0.50 $\pm$ 0.19 c
$E_L$ (mm d <sup>-1</sup> )	0.96 $\pm$ 0.43 ab	0.90 $\pm$ 0.33 ab	0.98 $\pm$ 0.36 ab	0.73 $\pm$ 0.25 c	0.93 $\pm$ 0.35 b	1.04 $\pm$ 0.41 a
$g_c$ (mm s <sup>-1</sup> )	1.96 $\pm$ 0.67 ab	1.61 $\pm$ 0.54 cd	2.04 $\pm$ 0.73 a	1.46 $\pm$ 0.55 d	1.81 $\pm$ 0.60 bc	1.90 $\pm$ 0.44 ab

Different letters next to numbers represent significantly different means between treatments ( $p < 0.05$ ).

### 3.2.2. Individual Tree and Stand-Level Transpiration

$E_t$  was the highest in June across all treatments, decreased slightly from July to September, and then decreased sharply in October due to rainfall events (Figure 5a). The interaction effect on  $E_t$  was statistically significant ( $p < 0.001$ ) (Table 2). At the same T1 treatment,  $E_t$  was significantly reduced by 15.34% ( $p < 0.001$ ) and 20.39% ( $p < 0.001$ ) at P1 and P2 compared to P0, respectively. However, there was no significant difference in  $E_t$  between pruning treatments ( $p > 0.05$ ) at the same T2 treatment (Figure 5b). Regardless of pruning treatments, thinning had a significant effect on reducing  $E_t$  ( $p < 0.001$ ) by 65.74% for T2P0 relative to T1P0, 62.65% for T2P1 relative to T1P1, and 54.26% for T2P2 relative to T1P2 (Figure 5b; Table 3).

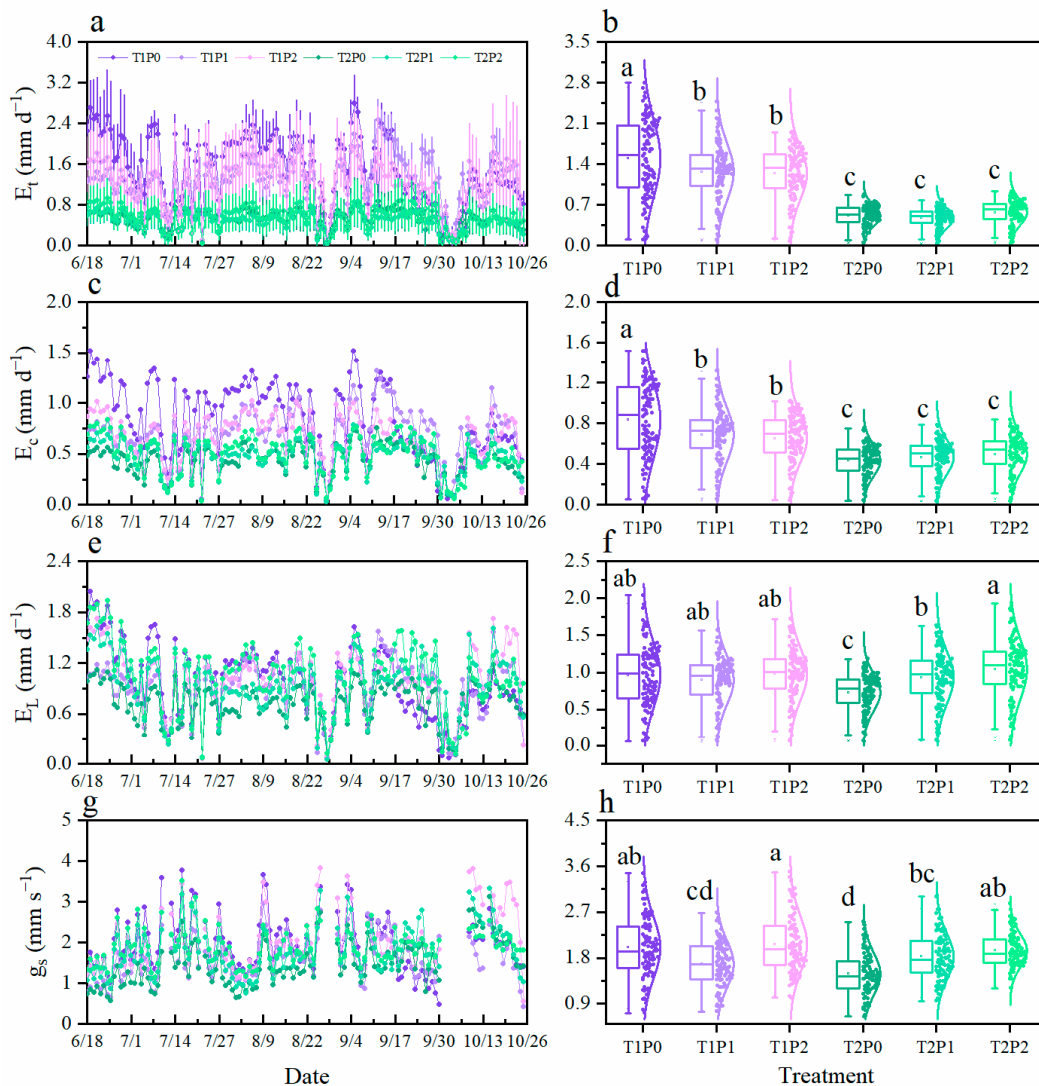


**Figure 5.** Seasonal dynamics of individual transpiration ( $E_t$ ), stand transpiration ( $E_c$ ), transpiration per unit leaf area ( $E_L$ ), and canopy conductance ( $g_c$ ) under different treatments (a,c,e,g). Box plots indicate the range of distributions, and the data points represent sample sizes of the treatments, which were fitted with normal curves (b,d,f,h). Different letters represent significantly different means between treatments ( $p < 0.05$ ).

The interaction effect on  $E_c$  was found to be significant ( $p < 0.001$ ) (Table 2). At the same T1 treatment,  $E_c$  was significantly reduced by 17.38% ( $p < 0.001$ ) and 21.70% ( $p < 0.001$ ) at P1 and P2 compared to P0, respectively. In the case of T2 treatment, there was no significant difference in  $E_c$  between pruning treatments ( $p > 0.05$ ) (Figure 5d). Regardless of pruning treatments, the thinning effect was found to reduce  $E_c$  significantly ( $p < 0.001$ ) by 47.89% for T2P0 relative to T1P0, 31.94% for T2P1 relative to T1P1, and 23.74% for T2P2 relative to T1P2 (Figure 5d). The total  $E_c$  of the treatments during the main growing period were 108.30, 89.48, 84.80, 56.43, 60.90, 64.67 mm, which accounted for 34.52%, 28.52%, 27.03%, 17.99%, 19.41%, 20.62% of rainfall, respectively.

### 3.2.3. Canopy Transpiration per Unit Leaf Area and Canopy Conductance

The results showed that the seasonal variations in  $E_L$  were relatively moderate (Figure 5e). Statistical analysis revealed that the interaction effect of thinning and pruning significantly influenced  $E_L$  ( $p < 0.001$ ) (Table 2). Specifically, in T2, P1 and P2 significantly increased  $E_L$  by 27.75% ( $p < 0.05$ ) and 43.21% ( $p < 0.001$ ) compared to P0 (Figure 5f). In the case of P0, T2 decreased  $E_L$  by 24.52% ( $p < 0.001$ ) compared to T1. Conversely, when P1

and P2 were applied, there was no significant difference in  $E_L$  between T1 and T2 ( $p > 0.05$ ) (Figure 5f; Table 3).

Seasonal changes in  $g_c$  were insignificant from the beginning of the measurements until mid-September for all treatments (Figure 5g). The interaction effect on  $g_c$  was found to be significant ( $p < 0.001$ ) (Table 2). In comparison to P0, P1 was found to be significantly reduced  $g_c$  by 18.02% ( $p < 0.001$ ), while there was no significant difference in  $g_c$  between P0 and P2 ( $p > 0.05$ ) at the same T1 treatment (Figure 5h). P1 and P2 significantly increased  $g_c$  by 23.73% ( $p < 0.001$ ) and 29.81% ( $p < 0.001$ ) compared to P0 at the same T2 treatment (Figure 5h; Table 3). Only in P0 was the  $g_c$  of T2 lower by 25.40% compared to T1 (Figure 5h).

### 3.3. Responses of Canopy Transpiration per Unit Leaf Area and Canopy Conductance to Environmental Variables

Daily  $E_L$  had a significantly positive relationship with  $VPD$ ,  $PAR$ , and  $ET_0$  ( $p < 0.001$ ) (Figure 6; Tables S1–S3).  $E_L$  was more affected by  $VPD$ ,  $PAR$ , and  $ET_0$  than the other atmospheric factors.  $T_{air}$ ,  $W_s$ , and  $\theta$  were not highly correlated with  $E_L$  for different treatments (Figure S4; Tables S4–S6). Additionally, it is noteworthy that the slope of the regression equations of  $E_L$  with  $VPD$ ,  $PAR$ , and  $ET_0$  decreased significantly in T1 while the slope increased significantly in T2 as pruning height increased (Figure 6; Table 4). Only in T1P0 did  $VPD$  explain a lower proportion of the variation in  $E_L$  than  $PAR$  and  $ET_0$  (67%, 70%, and 77%), respectively. For the other treatments,  $VPD$  was the main factor that explained the variation in  $E_L$  (greater than  $PAR$  and  $ET_0$ ) (Tables S1–S3).

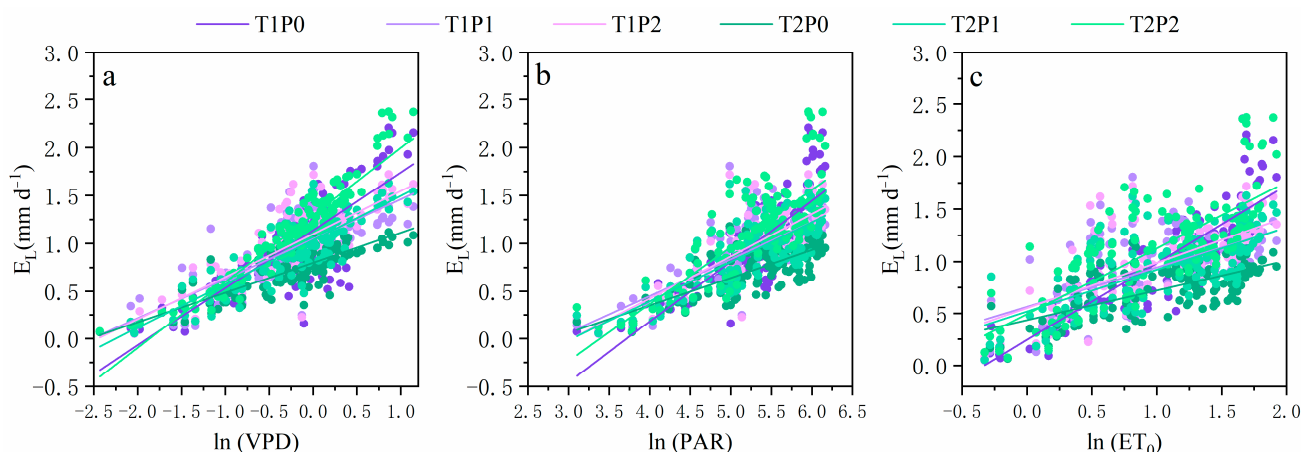


**Figure 6.** Response relationship between transpiration rate per unit leaf area ( $E_L$ ) and vapor pressure deficit ((a),  $\ln(VPD)$ ), photosynthetic active radiation ((b),  $\ln(PAR)$ ), and reference evapotranspiration ((c),  $\ln(ET_0)$ ) for different treatments.

**Table 4.** Test for slope between vapor pressure deficit ( $VPD$ ), photosynthetic active radiation ( $PAR$ ), reference evapotranspiration ( $ET_0$ ), and transpiration rate per unit leaf area ( $E_L$ ) among different treatments.

Treatments	VPD		PAR		ET <sub>0</sub>	
	Slope	<i>p</i>	Slope	<i>p</i>	Slope	<i>p</i>
T1P0	0.739 a	<0.001	0.757 a	<0.001	0.842 a	<0.001
T2P2	0.535 b	<0.001	0.548 b	<0.001	0.610 b	<0.001
T1P2	0.549 b	<0.001	0.563 b	<0.001	0.626 b	<0.001
T2P1	0.383 c	<0.001	0.393 c	<0.001	0.437 c	<0.001
T1P1	0.538 b	<0.001	0.551 b	<0.001	0.613 b	<0.001
T2P0	0.736 a	<0.001	0.754 a	<0.001	0.839 a	<0.001

Different letters next to numbers represent significantly different means between treatments ( $p < 0.05$ ).

The daily mean  $g_c$  exhibited a higher sensitivity to  $VPD$  than  $PAR$  in all treatments, with a significant decrease in  $g_c$  as  $VPD$  increased ( $p < 0.001$ ) (Figures 7 and S5; Tables S7 and S8). Boundary line analysis revealed no significant difference in  $m$  between T1P0 and T1P1, T2P0 and T2P1, nor T1P0 and T2P0 ( $p > 0.05$ ), but there was a significant difference in  $m$  between the other treatments ( $p < 0.05$ ) (Figure 7b; Table S7). Meanwhile, there was no significant difference in  $g_{cr}$  between T1P0 and T1P2, nor T1P2 and T2P2 ( $p > 0.05$ ), but there was a significant difference in  $g_{cr}$  the other treatments ( $p < 0.05$ ) (Figure 7b; Table S7). The strong linear relationship between  $m$  and  $g_{cr}$  across treatments, with approximately 0.6 slopes (Figure 7b), indicated an isohydric water strategy across all treatments.

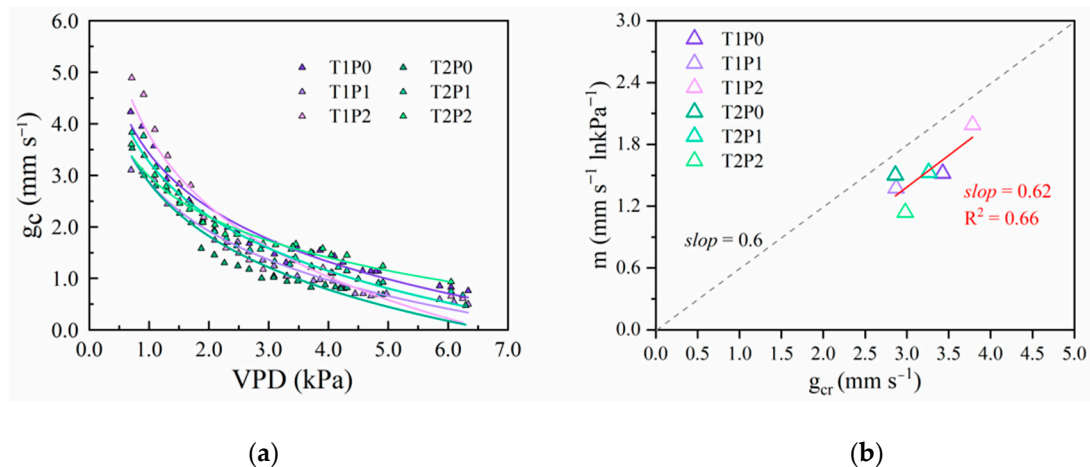


**Figure 7.** Logarithmic function of canopy conductance ( $g_c$ ) and vapor pressure deficit ( $VPD$ ) (a), the sensitivity of  $g_c$  to  $VPD$  and maximum canopy conductance ( $g_{cr}$ ) under different treatments (b).

### 3.4. Stand Water Use Efficiency in Different Rainfall Periods

During the study period, stand  $WUE$  was significantly higher ( $p > 0.05$ ) in the T2P0 treatment compared to the other treatments (Figure 8b). However,  $BAI$  showed no significant differences ( $p > 0.05$ ) among all treatments (Figure 8a) but differed in different rainfall periods (Table 5). The total rainfall from 18 June to 22 August (wet summer) was 218.44 mm (Figure 8c). During this period,  $BAI$  was positively correlated with  $E_c$  for T1P0, T2P1, and T2P2 and negatively correlated with  $E_c$  for T1P1, T1P2, and T2P0 (Figure 9a). Additionally,  $WUE$  was significantly higher for T2P0 than the other treatments ( $p < 0.05$ ) (Figure 9c).  $BAI$  showed a significant difference among treatments ( $p < 0.05$ ), with T2P0 and T1P0 each having significantly higher  $BAI$  than other treatments ( $p < 0.05$ ) (Figure 8c; Table 5). In terms of transpiration,  $E_c$  was significantly higher in T1P0 than in the other treatments ( $p < 0.05$ ), while it was significantly lower ( $p < 0.05$ ) in T2P0 than in T1P0 (Figure 8c).

During the dry autumn period from 23 August to 25 October, the rainfall was low at 95.25 mm (Figure 8c). In all treatments,  $BAI$  and  $E_c$  were positively correlated (Figure 9b), and there were no significant differences ( $p > 0.05$ ) in  $BAI$  among treatments (Table 5). T2P0 had the highest  $BAI$ , while T1P0 exhibited the lowest (Figure 8c). For  $E_c$ , no significant differences were noted ( $p > 0.05$ ) among pruning treatments under the same thinning treatment. However, T1P0 had significantly higher  $E_c$  than T2P0 ( $p < 0.05$ ) (Figure 8c).  $WUE$  was significantly higher in T2P0 than in both T1P0 ( $p < 0.05$ ) and T1P1 ( $p < 0.05$ ) (Figure 9c). Notably, the correlation coefficients between  $BAI$  and  $E_c$  were higher in all treatments during dry autumn than during wet summer, except for T1P1 and T2P1, even though precipitation during dry autumn was less than that during wet summer (Figure 9a,b). This suggests that the contribution of  $E_c$  to  $BAI$  was more significant in dry autumn than in wet summer.

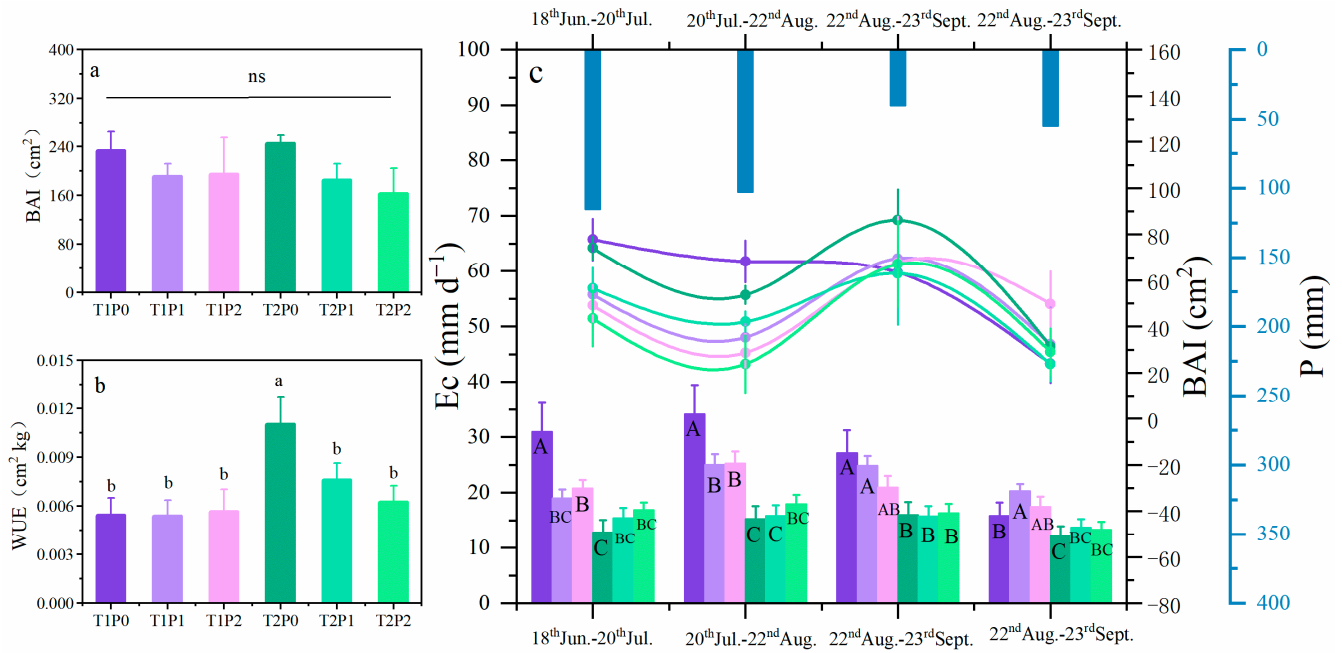


**Figure 8.** Analysis of total stand-scale basal area increment (BAI) (a), water use efficiency (WUE) (b), and differences between basal area increment (BAI) and transpiration ( $E_c$ ) in different precipitation periods under different thinning–pruning treatments (c). In (c), the bar located at the top represents the cumulative rainfall ( $P$ ) in each period; the bars located at the bottom represent the transpiration ( $E_c$ ) of T1P0, T1P1, T1P2, T2P0, T2P1, and T2P2 in each period, respectively; the curve located in the middle represents the change in basal area increment (BAI) in each period. Different uppercase letters and lowercase letters represent significantly different means between treatments in  $E_c$  and WUE ( $p < 0.05$ ), respectively.

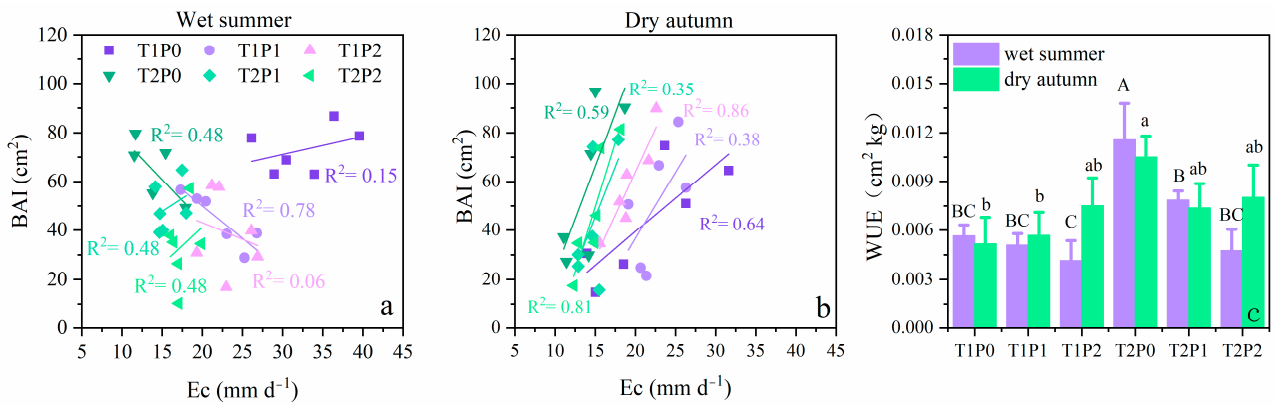


**Figure 9.** Differences in synergistic patterns of change in stand-scale basal area increment (BAI) and transpiration ( $E_c$ ) in wet summer (a) and dry autumn (b), i.e., differences in water use efficiency (WUE) under different thinning and pruning treatments (c). Different uppercase letters and lowercase letters represent significantly different means between treatments in wet summer and dry summer ( $p < 0.05$ ), respectively.



**Table 5.** Basal area increment (*BAI*) and leaf area index (*LAI*) at the stand scale under different thinning and pruning treatments in different precipitation periods.

Treatment	Wet Summer				Dry Autumn			
	18 June–20 July		20 July–22 August		22 August–23 September		23 September–25 October	
	<i>BAI</i>	<i>LAI</i>	<i>BAI</i>	<i>LAI</i>	<i>BAI</i>	<i>LAI</i>	<i>BAI</i>	<i>LAI</i>
T1P0	77.78 ± 8.96 a	0.85 ± 0.21 a	68.27 ± 9.02 a	0.96 ± 0.20 a	63.40 ± 11.96	0.82 ± 0.02 a	23.90 ± 8.19	0.80 ± 0.12 ab
T1P1	53.8 ± 2.47 abc	0.75 ± 0.10 ab	35.35 ± 5.61 bc	0.78 ± 0.10 ab	69.48 ± 13.68	0.77 ± 0.04 a	32.33 ± 15.96	0.73 ± 0.10 b
T1P2	49.07 ± 15.68 bc	0.71 ± 0.05 ab	28.69 ± 11.43 c	0.81 ± 0.05 abc	67.75 ± 22.45	0.55 ± 0.04 b	49.74 ± 14.18	0.55 ± 0.06 c
T2P0	74.08 ± 4.88 ab	0.61 ± 0.03 bc	53.71 ± 3.88 ab	0.67 ± 0.03 bcd	86.11 ± 13.17	0.55 ± 0.03 b	31.46 ± 5.09	0.91 ± 0.07 a
T2P1	56.45 ± 9.03 abc	0.51 ± 0.06 c	42.02 ± 4.37 bc	0.60 ± 0.06 cd	63 ± 22.18	0.44 ± 0.06 c	23.75 ± 7.33	0.45 ± 0.04 c
T2P2	43.43 ± 12.05 c	0.48 ± 0.07 c	23.77 ± 12.34 c	0.51 ± 0.07 d	67.06 ± 18.62	0.48 ± 0.04 bc	29.07 ± 10.04	0.46 ± 0.04 c

Different letters next to numbers represent significantly different means between treatments ( $p < 0.05$ ).

## 4. Discussion

### 4.1. Response Patterns of Individual Tree and Stand-Level Transpiration under Thinning and Pruning Treatments

Our study observed that the daily mean  $E_t$  and  $E_c$  decreased with different combined thinning and pruning treatments, indicating similar transpiration patterns at individual tree and stand levels (Figure 5a–d). This finding addresses the first scientific question of our study. In addition, regardless of pruning heights, T1 showed higher average daily transpiration compared to T2 (Figure 5d). This suggests that transpiration decreases with increasing thinning intensity, which is consistent with the findings of Forrester et al. [11], Guohui Wang et al. [74], Tsamir et al. [75], and Thibaud André-Alphonse et al. [39]. Two main factors contribute to these results. Firstly, the *LAI* was higher in T1 compared to T2 (Figure S1). The decline in transpiration with increasing thinning intensity can be attributed to the reduction in leaf area at both the individual tree and stand levels, a phenomenon supported by other studies that have also noted a decrease in transpiration with reduced stand leaf area [42,76]. Secondly, the reductions in stand basal area (*BA*) in T2, which resulted from thinning, were 10.21% (P0), 5.38% (P1), and 21.83% (P2) lower than T1. The reduction in stand transpiration was more significant relative to the percentage reduction in the stand density, which can be attributed to the reduction in transpiration of the individual tree level following thinning (Figure 5b). These findings differ from those of Timo Gebhardt et al. [19], where sap flow density rates decreased in both individual trees and stand with increasing thinning intensity (Figure 4a). Additionally, negative correlations between transpiration and thinning intensity have been observed in arid regions [41,77–79], but our study area experienced abundant rainfall. André-Alphonse et al. found variations in moisture conditions across different regions [39], leading to different relationships between transpiration and thinning intensity outcomes.

After pruning, Forrester et al. [11] found that trees exhibited increased efficiency in water and light use, increasing transpiration per unit leaf area. This pattern is consistent with the observed effects of pruning on transpiration in T2 (Figure 5f). Despite no significant difference in stand transpiration among all the pruning heights in T2 (Figure 5d), the number of leaves decreased after pruning (Figure S1), which would typically result in reduced transpiration. However, in T2, where the thinning intensity was higher, the remaining leaves exhibited greater transpiration per unit leaf area (P1 and P2) compared to P0 (Figure 5f), and  $J_m$  was higher also (Figure 4a). This aligns with the leaf compensation mechanism, where the photosynthetic and transpiration capacities of remaining leaves are enhanced after pruning [11,23,35,80]. This promotes transpiration at both the individual tree and stand levels. Contrastingly, in T1, which had a higher tree density, pruning did not increase the canopy conductance and transpiration rate per unit leaf area, resulting in a decrease in transpiration. This can be attributed to shaded foliage in the lower canopy of high-density stands causing self-thinning due to insufficient light conditions [10], and pruning does not induce a compensatory effect. These findings align with the studies by Chen et al. [35], Molina et al. [43], and Alcorn et al. [23].

#### 4.2. Response of Transpiration and Canopy Conductance to Environmental Factors

Different treatments change the response of  $E_L$  to climatic factors. Firstly, the  $E_L$  of T1P0 and T2P2 had the highest response to  $VPD$ ,  $PAR$ , and  $ET_0$  (Figure 6). That was because the  $g_c$  did not decrease rapidly with increasing  $VPD$  and remained open at high levels (Figure 7a). Pruning had an opposite effect on the stands of different densities of  $E_L$ . It showed a negative effect on dense stands and a promotive effect on sparse stands. This suggests that we should consider the role of stand density when researching the effect of pruning on  $E_L$ , since the reduction in  $E_L$  response to the environment caused by thinning may be eliminated by pruning effects. Secondly, different treatments altered the proportion of environmental factors to explain the variation in  $E_L$ . The explanation of variation in  $E_L$  by  $VPD$  was the lowest only in T1P0 and the highest in the other treatments. This may be due to the fact that pruning and thinning reduce the  $LAI$  of the stand (Figure S1), which tends to make the environment drier and warmer, increasing the limitations on evapotranspiration by the  $VPD$ .

$g_c$  plays a critical role in governing canopy transpiration. During periods of elevated  $VPD$ , stomatal closure becomes essential to preventing excessive water loss, maintaining leaf water potential above a critical threshold, and averting xylem cavitation or dysfunction [81–83]. Our study found that  $g_c$  was more strongly correlated to  $VPD$  than to  $PAR$  (Figures 7 and S5), which is consistent with Du et al. [32]. This correlation is attributed to the relatively low stand density observed across all treatments, allowing the entire canopy to receive more sunlight and subsequently reducing the saturation threshold for  $PAR$  [34,37]. This suggests that  $VPD$  significantly influences stomatal regulation and transpiration in poplar trees [30,32].

The sensitivity of  $g_c$  to  $VPD$  is related to  $g_{cr}$  [69]. In our study, T1P2 exhibited high  $g_c$  under low  $VPD$  conditions, indicating stomatal closure (evidenced by high  $m$  values) in response to increased  $VPD$  (Figure 7). This suggests that stomata are more responsive to dry air under T1P2. They are more responsive to stimuli, which may cause stomatal closure. Isohydric tree species, employing an active control of  $g_c$ , maximize carbon uptake under low  $VPD$  conditions, thereby avoiding the risk of wilting due to soil drought. This tree feature, regulating the leaf minimum water potential to circumvent xylem cavitation, is reflected in the  $m/g_{cr}$  ratio [84]. Most species typically exhibit  $m/g_{cr}$  values of 0.6, indicative of relatively stringent stomatal regulation and a low ratio of boundary layer conductance to canopy conductance [69,71,85]. Larger canopy exposures resulted in changes in  $VPD$  and boundary layer conductance, which increased with increasing tree spacing due to increased wind speed [86]. In our experiments, the value of  $m/g_{cr}$  was less than 0.6 for all treatments, which was due to the fact that the average value of the decoupling coefficient ( $\Omega$ ) for all treatments was less than 0.1 (0.001–0.23), indicating that there was a high degree of canopy coupling to the atmosphere. This suggests that the effect of boundary layer conductance was very small [69].

Stomatal regulation of transpiration can be flexible [87]. A three-year study conducted in an arid zone demonstrated that poplars can alter transpiration by actively controlling stomata in response to varying environmental conditions [32]. In this study, *P. tomentosa* trees showed differences in  $g_{cr}$  under different pruning heights in T2, which resulted in the variation in the magnitude of transpiration rate per unit leaf area (Figures 5f and 7b). In T2, the pruning treatment of 3 m (P1) had no significant effect on the  $m$ , but  $g_{cr}$  was significantly increased in comparison to P0. The pruning treatment of 4 m (P2) significantly decreased the  $m$  and increased  $g_{cr}$ . This suggests that in lower density stands (T2), the increase in  $g_{cr}$  is the main reason for the increase in  $E_L$  after pruning treatment. Similar conclusions were obtained by Chen et al. [35] in a study on the influence of branch removal on  $m$  and  $g_{cr}$ . Meanwhile, in lower density stands, the pruning-induced significant reduction in the number of more-light-exposed leaves in the lower crowns of the trees may account for the reduced response of  $g_c$  to  $VPD$ . In T1, both pruning treatments of 3 m (P1) significantly decreased  $m$  and  $g_{cr}$ , and pruning treatments of 4 m (P2) significantly increased  $m$  but had no effect on  $g_{cr}$ . Although pruning treatments could produce significant changes in  $m$  and

$g_{cr}$  in the higher density stands (T1), the difference between the two did not cause changes in  $E_L$ . In addition to this, this suggests that in higher density stands, only pruning away a sufficient proportion of lower canopy shading leaves (4 m) can improve the  $g_c$  response to  $VPD$ . The results of  $m$  and  $g_{cr}$  may be biased due to the limited sample size [32]. The results indicate that *P. tomentosa* can flexibly regulate its transpiration to maintain its growth and survival, which answers the second scientific question.

#### 4.3. Water Use Efficiency and Basal Area Increment

Poplar is a fast-growing species sensitive to the environment, and short-term moisture changes can affect its growth [88,89]. Thinning can alter the microclimate of the stand and its  $WUE$  [48]. This study found that stand  $WUE$  was increased after thinning, with T2P0 showing a statistically significant increase compared to the other treatments. This answers the third scientific question of this study. Notably, the differences in  $WUE$  among the thinning and pruning treatments were more pronounced at the monthly scale and were associated with rainfall. However, the  $BAI$  of the stands did not show significant differences at the annual level (Figure 8a). It also differed significantly at different monthly levels (Figure 8c; Table 5). Thus, the changes in  $WUE$  and  $BAI$  of poplar stands should be investigated under different rainfall conditions.

Studies have presented conflicting findings on stand  $WUE$  in relation to rainfall, with some reporting an increase in  $WUE$  as rainfall decreases [48] and others observing a decrease as rainfall increases [90]. In this study, the  $WUE$  of T2P0 was significantly higher than other treatments during the rainy season, while there was no significant difference between T2P0, T2P1, T2P2, and T1P2 in the dry season. Additionally, stand diameter growth showed uncertainty under varying moisture conditions. For instance, He et al. [91] found that reduced precipitation led to lower growth, while Xue et al. [92] noted that excessive precipitation also resulted in reduced radial growth. In contrast, Rahman et al. [93] observed opposing effects of precipitation on radial growth at different rainfall periods. In our study, a significant decreasing trend in  $BAI$  was observed with increasing pruning intensity under the same thinning treatment (Table 5) because pruning reduces the canopy and decreases the  $LAI$  of the stand (Figure S1; Table 5), aligning with findings by Huang et al. [94]. However,  $BAI$  did not exhibit any difference across all treatments in the dry season (Table 5).

Since  $WUE$  is influenced by both  $E_c$  and  $BAI$ , and both factors are impacted by rainfall [29,46], we further explored the relationship between  $E_c$  and  $BAI$  under different rainfall conditions (Figure 9a,b). In the wet summer, negative correlations were observed between  $E_c$  and  $BAI$  in T1P1, T1P2, and T2P0, while the remaining treatments showed an increase in  $BAI$  with rising  $E_c$  (Figure 9a). This phenomenon was attributed to a decrease in  $BAI$  with rising  $E_c$  (Table 5; Figure 8c). In the dry autumn,  $E_c$  and  $BAI$  had a positive correlation in all treatments (Figure 9b). This aligns with the findings of Li et al. [30], suggesting that the contribution of transpiration to growth was further enhanced under water deficit conditions.

From a plantation management perspective, the  $BAI$  of all the thinning and pruning treatments increased during the late growing season (22 August to 23 September) compared to T1P0. This suggests that thinning and pruning can promote tree growth and prolong the growth period of *P. tomentosa*. Although there was no statistically significant difference in the  $BAI$  among treatments at the end of the season, the  $BAI$  of T1P2, T2P1, and T2P0 was higher due to higher  $g_c$  and  $WUE$  in the late growing season (Figures 5g and 9c). It should be noted that these findings were obtained in one growing season, and further research at longer time scales is needed to fully understand the effects of poplar sensitivity to environmental changes and plantation management.

## 5. Conclusions

In this paper, we systematically investigated the response of *P. tomentosa* plantations'  $J_s$ ,  $E_c$ ,  $E_L$ ,  $g_c$ ,  $WUE$ , and  $BAI$  of to different thinning and pruning intensities. Six treatments

with two densities and three pruning heights were established, and the results show that the transpiration patterns were consistent at both individual tree and stand levels. We observed that stand transpiration and growth varied across treatments, and that these differences were related to the rainfall period within the year. In T1, thinning and pruning reduced  $E_c$  and decreased the sensitivity of tree transpiration to climate, while in the sparse plantation, T2, the combination of thinning and pruning promoted  $E_L$  and  $g_s$  but increased the sensitivity of tree transpiration to climate. The stomatal regulation of *P. tomentosa* under different treatments was flexible, and the pruning effects significantly reduced  $WUE$  in T2. Overall, T2P0 had the highest  $WUE$ , and T1P0 had the lowest. Moreover, there were significant differences in  $E_c$  and  $BAI$  among the treatments under different rainfall conditions, with  $E_c$  having a more significant impact on  $BAI$  during the dry autumn. Thinning and pruning moderated the decline in plantation growth at the end of the growing season due to the effect of improving canopy conductance and water use efficiency.

In conclusion, thinning and pruning can promote the growth of *P. tomentosa* plantations by changing their water utilization capacity, but local water conditions should be considered when managing these plantations. Long-term studies are necessary to obtain the optimal plantation management plan for the entire cycle.

**Supplementary Materials:** The following supporting information can be downloaded at: <https://www.mdpi.com/article/10.3390/f15030536/s1>. Figure S1. Seasonal variations of daily values of leaf area index ( $LAI$ ). Figure S2. The frequency distribution of stem diameters at breast height ( $DBH$ ) for T1P0, T1P1, T1P2, T2P0, T2P1, and T2P2 is presented in figures (a), (b), (c), (d), (e), and (f) respectively. Figure S3. Logarithmic function of canopy conductance ( $g_c$ ) and vapor pressure deficit ( $VPD$ ) before BLA. Figure S4. Response relationship between transpiration rate per unit leaf area ( $E_L$ ) and air temperature (a,  $T_{air}$ ), wind speed at 2 m height (b,  $W_s$ ), soil water content (c,  $\theta$ ) at the depths of 20 cm soil layer for different treatments. Figure S5. Response relationship between canopy conductance ( $g_c$ ) and photosynthetic active radiation ( $PAR$ ) for different treatments. Table S1. Linear regression functional equation for transpiration rate per unit leaf area ( $E_L$ ) and vapor pressure deficit ( $\ln VPD$ ). Table S2. Linear regression functional equation for transpiration rate per unit leaf area ( $E_L$ ) and photosynthetic active radiation ( $\ln PAR$ ). Table S3. Linear regression functional equation for transpiration rate per unit leaf area ( $E_L$ ) and reference evapotranspiration ( $\ln ET_0$ ). Table S4. Linear regression functional equation for transpiration rate per unit leaf area ( $E_L$ ) and air temperature ( $T_{air}$ ). Table S5. Linear regression functional equation for transpiration rate per unit leaf area ( $E_L$ ) and wind speed ( $W_s$ ). Table S6. Linear regression functional equation for transpiration rate per unit leaf area ( $E_L$ ) and soil water content ( $\theta$ ). Table S7. Logarithmic function of canopy conductance ( $g_c$ ) and vapor pressure deficit ( $VPD$ ) and their function after the boundary line analysis (BLA). Table S8. Linear regression functional equation for canopy conductance ( $g_c$ ) and photosynthetic active radiation ( $PAR$ ).

**Author Contributions:** Conceptualization, Y.L. (Yan Liu) and J.D.; formal analysis, Y.L. (Yan Liu); investigation, resources, data curation, Y.L. (Yan Liu), S.Q., Z.F., Z.L., Q.T., Y.X. and X.Z.; writing—original draft preparation, Y.L.; writing—review and editing, visualization, Y.L. (Yan Liu), Y.L. (Yadong Liu) and B.X.; supervision, project administration, funding acquisition, J.D. research forest management, C.W. All authors have read and agreed to the published version of the manuscript.

**Funding:** This research was funded by the National Key Research and Development Program of China (2021YFD2201203), the Nature Science Foundation of China (31971640).

**Data Availability Statement:** The data presented in this paper are available on request from the corresponding author.

**Acknowledgments:** The authors appreciate the support and assistance given by the staff of Wen County Forestry Science Research Institution in Henan Province during the field trials.

**Conflicts of Interest:** The authors declare no conflicts of interest.

## References

1. FAO. *Global Forest Resources Assessment 2020*; FAO: Rome, Italy, 2020.
2. Bastin, J.; Finegold, Y.; Garcia, C.; Mollicone, D.; Rezende, M.; Routh, D.; Rezende, M.; Routh, D.; Zohner, C.M.; Crowther, T.W. The global tree restoration potential. *Sci. Total Environ.* **2019**, *365*, 76–79. [[CrossRef](#)]



3. Cabbage, F.; Koesbandana, S.; Donagh, P.M.; Rubilar, R.; Balmelli, G.; Olmos, V.M.; Torre, R.D.; Murara, M.; Hoeflich, V.A.; Kotze, H.; et al. Global timber investments, wood costs, regulation, and risk. *Biomass Bioenerg.* **2010**, *34*, 1667–1678. [[CrossRef](#)]
4. National Forestry and Grassland Administration. *China Forest Resources Report*; National Forestry and Grassland Administration: Beijing, China, 2019.
5. IPCC. AR6 Synthesis Report: Climate Change 2023. Available online: <https://www.ipcc.ch/report/sixth-assessment-report-cycle/> (accessed on 1 September 2023).
6. McDowell, N.G.; Allen, C.D. Darcy's law predicts widespread forest mortality under climate warming. *Nat. Clim. Chang.* **2015**, *5*, 669–672. [[CrossRef](#)]
7. Allen, C.D.; Macalady, A.K.; Chenchouni, H.; Bachelet, D.; McDowell, N.; Venetier, M.; Kitzberger, T.; Rigling, A.; Breshears, D.D.; Hogg, E.H.; et al. A global overview of drought and heat-induced tree mortality reveals emerging climate change risks for forests. *For. Ecol. Manag.* **2010**, *259*, 660–684. [[CrossRef](#)]
8. Martínez-Vilalta, J.; Pinol, J. Drought-induced mortality and hydraulic architecture in pine populations of the NE Iberian Peninsula. *For. Ecol. Manag.* **2002**, *161*, 247–256. [[CrossRef](#)]
9. Forrester, D.I.; Collopy, J.J.; Beadle, C.L.; Baker, T.G. Effect of thinning, pruning and nitrogen fertiliser application on light interception and light-use efficiency in a young *Eucalyptus nitens* plantation. *For. Ecol. Manag.* **2013**, *288*, 21–30. [[CrossRef](#)]
10. Forrester, D.I. Growth responses to thinning, pruning and fertiliser application in *Eucalyptus* plantations: A review of their production ecology and interactions. *For. Ecol. Manag.* **2013**, *310*, 336–347. [[CrossRef](#)]
11. Forrester, D.I.; Collopy, J.J.; Beadle, C.L.; Warren, C.R.; Baker, T.G. Effect of thinning, pruning and nitrogen fertiliser application on transpiration, photosynthesis and water-use efficiency in a young *Eucalyptus nitens* plantation. *For. Ecol. Manag.* **2012**, *266*, 286–300. [[CrossRef](#)]
12. Eyles, A.; Pinkard, E.A.; Mohammed, C. Shifts in biomass and resource allocation patterns following defoliation in *Eucalyptus globulus* growing with varying water and nutrient supplies. *Tree Physiol.* **2009**, *29*, 753–764. [[CrossRef](#)]
13. Wang, C.S.; Zeng, J. Research advances in forest tree pruning. *World For. Res.* **2016**, *29*, 65–70, (with Abstract in English).
14. Ma, L.; Wang, X.; Gao, Z.; Wang, Y.; Nie, Z.; Liu, X. Canopy pruning as a strategy for saving water in a dry land jujube plantation in a loess hilly region of China. *Agric. Water Manag.* **2019**, *216*, 436–443. [[CrossRef](#)]
15. Park, J.; Kim, T.; Moon, M.; Cho, S.; Ryu, D.; Kim, H.S. Effects of thinning intensities on tree water use, growth, and resultant water use efficiency of 50-year-old *Pinus koraiensis* forest over four years. *For. Ecol. Manag.* **2018**, *408*, 121–128. [[CrossRef](#)]
16. Fernandes, T.J.G.; Del Campo, A.D.; Herrera, R.; Molina, A.J. Simultaneous assessment, through sap flow and stable isotopes, of water use efficiency (WUE) in thinned pines shows improvement in growth, tree-climate sensitivity and WUE, but not in WUEi. *For. Ecol. Manag.* **2016**, *361*, 298–308. [[CrossRef](#)]
17. Sohn, J.A.; Saha, S.; Bauhus, J. Potential of forest thinning to mitigate drought stress: A meta-analysis. *For. Ecol. Manag.* **2016**, *380*, 261–273. [[CrossRef](#)]
18. del Campo, A.D.; González-Sanchis, M.; García-Prats, A.; Ceacero, C.J.; Lull, C. The impact of adaptive forest management on water fluxes and growth dynamics in a water-limited low-biomass oak coppice. *Agric. For. Meteorol.* **2019**, *264*, 266–282. [[CrossRef](#)]
19. Gebhardt, T.; Häberle, K.; Matyssek, R.; Schulz, C.; Ammer, C. The more, the better? Water relations of Norway spruce stands after progressive thinning. *Agric. For. Meteorol.* **2014**, *197*, 235–243. [[CrossRef](#)]
20. Wang, Y.; del Campo, A.D.; Wei, X.; Winkler, R.; Liu, W.; Li, Q. Responses of forest carbon and water coupling to thinning treatments from leaf to stand scales in a young montane pine forest. *Carbon. Bal. Manag.* **2020**, *15*, 1. [[CrossRef](#)]
21. Wang, Y.; Wei, X.; del Campo, A.D.; Winkler, R.; Wu, J.; Li, Q.; Liu, W. Juvenile thinning can effectively mitigate the effects of drought on tree growth and water consumption in a young *Pinus contorta* stand in the interior of British Columbia, Canada. *For. Ecol. Manag.* **2019**, *454*, 117667. [[CrossRef](#)]
22. Lechuga, V.; Carraro, V.; Viñepla, B.; Carreira, J.A.; Linares, J.C. Managing drought-sensitive forests under global change. Low competition enhances long-term growth and water uptake in *Abies pinsapo*. *For. Ecol. Manag.* **2017**, *406*, 72–82. [[CrossRef](#)]
23. Alcorn, P.J.; Forrester, D.I.; Thomas, D.S.; James, R.; Smith, R.B.; Nicotra, A.B.; Bauhus, J. Changes in Whole-Tree Water Use Following Live-Crown Pruning in Young Plantation-Grown *Eucalyptus pilularis* and *Eucalyptus cloeziana*. *Forests* **2013**, *4*, 106–121. [[CrossRef](#)]
24. Moreno-Fernández, D.; Sánchez-González, M.; Álvarez-González, J.G.; Hevia, A.; Majada, J.P.; Canellas, I.; Gea-Izquierdo, G. Response to the interaction of thinning and pruning of pine species in Mediterranean mountains. *Eur. J. Forest. Res.* **2014**, *133*, 833–843. [[CrossRef](#)]
25. Forrester, D.I.; Medhurst, J.L.; Wood, M.; Beadle, C.L.; Valencia, J.C. Growth and physiological responses to silviculture for producing solid-wood products from *Eucalyptus* plantations: An Australian perspective. *For. Ecol. Manag.* **2010**, *259*, 1819–1835. [[CrossRef](#)]
26. Alcorn, P.J.; Bauhus, J.; Thomas, D.S.; James, R.N.; Smith, R.B.; Nicotra, A.B. Photosynthetic response to green crown pruning in young plantation-grown *Eucalyptus pilularis* and *E. cloeziana*. *For. Ecol. Manag.* **2008**, *255*, 3827–3838. [[CrossRef](#)]
27. Forrester, D.I.; Collopy, J.J.; Beadle, C.L.; Baker, T.G. Interactive effects of simultaneously applied thinning, pruning and fertiliser application treatments on growth, biomass production and crown architecture in a young *Eucalyptus nitens* plantation. *For. Ecol. Manag.* **2012**, *267*, 104–116. [[CrossRef](#)]



28. Song, L.; Zhu, J.; Zheng, X.; Wang, K.; Lü, L.; Zhang, X.; Hao, G. Transpiration and canopy conductance dynamics of *Pinus sylvestris* var. *mongolica* in its natural range and in an introduced region in the sandy plains of Northern China. *Agric. For. Meteorol.* **2020**, *281*, 107830. [[CrossRef](#)]
29. Song, L.; Zhu, J.; Zheng, X.; Wang, K.; Zhang, J.; Hao, G.; Wang, G.; Liu, J. Comparison of canopy transpiration between *Pinus sylvestris* var. *mongolica* and *Pinus tabuliformis* plantations in a semiarid sandy region of Northeast China. *Agric. For. Meteorol.* **2022**, *314*, 108784. [[CrossRef](#)]
30. Li, D.D.; Liu, J.; Verhoef, A.; Xi, B.Y.; Hernandez-Santana, V. Understanding the relationship between biomass production and water use of *Populus tomentosa* trees throughout an entire short-rotation. *Agric. Water Manag.* **2021**, *246*, 106710. [[CrossRef](#)]
31. Oogathoo, S.; Houle, D.; Duchesne, L.; Kneeshaw, D. Vapour pressure deficit and solar radiation are the major drivers of transpiration of balsam fir and black spruce tree species in humid boreal regions, even during a short-term drought. *Agric. For. Meteorol.* **2020**, *291*, 108063. [[CrossRef](#)]
32. Du, J.; Dai, X.; Huo, Z.; Wang, X.; Wang, S.; Wang, C.; Zhang, C.; Huang, G. Stand transpiration and canopy conductance dynamics of *Populus popularis* under varying water availability in an arid area. *Sci. Total Environ.* **2023**, *892*, 164397. [[CrossRef](#)]
33. López, J.; Way, D.A.; Sadok, W. Systemic effects of rising atmospheric vapor pressure deficit on plant physiology and productivity. *Glob. Chang. Biol.* **2021**, *27*, 1704–1720. [[CrossRef](#)] [[PubMed](#)]
34. Naithani, K.J.; Ewers, B.E.; Pendall, E. Sap flux-scaled transpiration and stomatal conductance response to soil and atmospheric drought in a semi-arid sagebrush ecosystem. *J. Hydrol.* **2012**, *464*, 176–185. [[CrossRef](#)]
35. Chen, D.; Wang, Y.; Wang, X.; Nie, Z.; Gao, Z.; Zhang, L. Effects of branch removal on water use of rain-fed jujube (*Ziziphus jujuba* Mill.) plantations in Chinese semiarid Loess Plateau region. *Agric. Water Manag.* **2016**, *178*, 258–270. [[CrossRef](#)]
36. Zhao, X.; Li, X.; Hu, W.; Liu, J.; Di, N.; Duan, J.; Li, D.; Liu, Y.; Guo, Y.; Wang, A.; et al. Long-term variation of the sap flow to tree diameter relation in a temperate poplar forest. *J. Hydrol.* **2023**, *618*, 129189. [[CrossRef](#)]
37. Granier, A.; Huc, R.; Barigah, S.T. Transpiration of natural rain forest and its dependence on climatic factors. *Agric. For. Meteorol.* **1996**, *78*, 19–29. [[CrossRef](#)]
38. Binkley, D.; Campoe, O.C.; Gspaltl, M.; Forrester, D.I. Light absorption and use efficiency in forests: Why patterns differ for trees and stands. *Agric. Water Manag.* **2013**, *288*, 5–13. [[CrossRef](#)]
39. André-Alphonse, T.; Mekontchou, C.G.; Rochon, P.; Doyon, F.; Maheu, A. Comparing the influence of thinning treatments with low to high residual basal area on red maple transpiration in a temperate mixed forest. *For. Ecol. Manag.* **2023**, *534*, 5–13. [[CrossRef](#)]
40. Liu, X.; Sun, G.; Mitra, B.; Noormets, A.; Gavazzi, M.J.; Domec, J.; Hallema, D.W.; Li, J.; Fang, Y.; King, J.S.; et al. Drought and thinning have limited impacts on evapotranspiration in a managed pine plantation on the southeastern United States coastal plain. *Agric. For. Meteorol.* **2018**, *262*, 14–23. [[CrossRef](#)]
41. del Campo, A.D.; Fernandes, T.J.; Molina, A. Hydrology-oriented (adaptive) silviculture in a semiarid pine plantation: How much can be modified the water cycle through forest management? *Eur. J. For. Res.* **2014**, *133*, 879–894. [[CrossRef](#)]
42. Moreno, G.; Cubera, E. Impact of stand density on water status and leaf gas exchange in *Quercus ilex*. *For. Ecol. Manag.* **2008**, *254*, 74–84. [[CrossRef](#)]
43. Molina, A.J.; Aranda, X.; Llorens, P.; Galindo, A.; Biel, C. Sap flow of a wild cherry tree plantation growing under Mediterranean conditions: Assessing the role of environmental conditions on canopy conductance and the effect of branch pruning on water productivity. *Agric. Water Manag.* **2019**, *218*, 222–233. [[CrossRef](#)]
44. Hubbard, R.M.; Stape, J.; Ryan, M.G.; Almeida, A.C.; Rojas, J. Effects of irrigation on water use and water use efficiency in two fast growing *Eucalyptus* plantations. *For. Ecol. Manag.* **2010**, *259*, 1714–1721. [[CrossRef](#)]
45. Dye, P.J. Water use efficiency in South African *Eucalyptus* plantations: A review. *S. Afr. For. J.* **2000**, *189*, 17–26.
46. del Campo, A.D.; Otsuki, K.; Serengil, Y.; Blanco, J.A.; Yousefpour, R.; Wei, X. A global synthesis on the effects of thinning on hydrological processes: Implications for forest management. *For. Ecol. Manag.* **2022**, *519*, 120324. [[CrossRef](#)]
47. Niccoli, F.; Pelleri, F.; Manetti, M.C.; Sansone, D.; Battipaglia, G. Effects of thinning intensity on productivity and water use efficiency of *Quercus robur* L. *For. Ecol. Manag.* **2020**, *473*, 118282. [[CrossRef](#)]
48. Gavinet, J.; Ourcival, J.; Limousin, J. Rainfall exclusion and thinning can alter the relationships between forest functioning and drought. *New Phytol.* **2019**, *223*, 1267–1279. [[CrossRef](#)]
49. Nelson, K.N.; Barnard, J.C.; Massingham, P.M.; Crotteau, J.S. Tree pruning improves tree form but not understory plant production in mixed stands of Sitka spruce and western hemlock, USA. *Forestry* **2023**, *97*, 309–318. [[CrossRef](#)]
50. Missanjo, E.; Kamanga-Thole, G. Effect of first thinning and pruning on the individual growth of *Pinus patula* tree species. *J. For. Res.* **2015**, *26*, 827–831. [[CrossRef](#)]
51. Reventlow, D.O.J.; Nord-Larsen, T.; Skovsgaard, J.P. Pre-commercial thinning in naturally regenerated stands of European beech (*Fagus sylvatica* L.): Effects of thinning pattern, stand density and pruning on tree growth and stem quality. *Forestry* **2019**, *92*, 120–132. [[CrossRef](#)]
52. Campbell, G.S.; Norman, J.M. *An Introduction to Environmental Biophysics*, 2nd ed.; Springer: New York, NY, USA, 1998.
53. Allen, R.G.; Pereira, L.S.; Raes, D.; Smith, M. *Crop Evapotranspiration. Guidelines for Computing Crop Water Requirements*; Rome Irrigation and drainage paper 56; FAO: Roma, Italy, 1998.
54. Granier, A. Evaluation of transpiration in a Douglas-fir stand by means of sap flow measurements. *Tree Physiol.* **1987**, *3*, 309–320. [[CrossRef](#)] [[PubMed](#)]

55. Lopez, J.G.; Licata, J.; Pypker, T.; Asbjornsen, H. Effects of heater wattage on sap flux density estimates using an improved tree-cut experiment. *Tree Physiol.* **2019**, *39*, 679–693.
56. Wiedemann, A.; Maranon-Jimenez, S.; Rebmann, C.; Herbst, M.; Cuntz, M. An empirical study of the wound effect on sap flux density measured with thermal dissipation probes. *Tree Physiol.* **2016**, *36*, 1471–1484. [[CrossRef](#)] [[PubMed](#)]
57. Clearwater, M.J.; Meinzer, F.C.; Andrade, J.L.; Goldstein, G.; Holbrook, N.M. Potential errors in measurement of nonuniform sap flow using heat dissipation probes. *Tree Physiol.* **1999**, *19*, 681–687. [[CrossRef](#)] [[PubMed](#)]
58. Flo, V.; Martinez-Vilalta, J.; Steppe, K.; Schuldt, B.; Poyatos, R. A synthesis of bias and uncertainty in sap flow methods. *Agric. For. Meteorol.* **2019**, *271*, 362–374. [[CrossRef](#)]
59. Fuchs, S.; Leuschner, C.; Link, R.; Coners, H.; Schuldt, B. Calibration and comparison of thermal dissipation, heat ratio and heat field deformation sap flow probes for diffuse-porous trees. *Agric. For. Meteorol.* **2017**, *244–245*, 151–161. [[CrossRef](#)]
60. Li, G.D.; Jia, L.M.; Fu, F.Z. Comparison on the whole-tree water use of hybrid triploid of Chinese white poplar between the whole tree potometer and thermal dissipation probe. *China For. Sci. Technol.* **2014**, *28*, 41–44.
61. Li, G.D.; Jia, L.M.; Fu, F.Z.; Xi, B.Y.; Wang, Y. Stem sap flow in different measurement positions of triploid *Populus tomentosa*. *Acta Bot. Boreas. Occident. Sin.* **2010**, *30*, 1209–1218, (in Chinese with English Abstract).
62. Song, L.; Zhu, J.J.; Zhang, T.; Wang, K.; Wang, G.C.; Liu, J.H. Higher canopy transpiration rates induced dieback in poplar (*Populus × xiaozhuanica*) plantations in a semiarid sandy region of Northeast China. *Agric. Water Manag.* **2021**, *243*, 106414. [[CrossRef](#)]
63. Shen, Q.; Gao, G.; Fu, B.; Lü, Y. Sap flow and water use sources of shelter-belt trees in an arid inland river basin of Northwest China. *Ecohydrology* **2015**, *8*, 1446–1458. [[CrossRef](#)]
64. Kumagai, T.; Nagasawa, H.; Mabuchi, T.; Ohsaki, S.; Kubota, K.; Kogi, K.; Utsumi, Y.; Koga, S.; Otsuki, K. Sources of error in estimating stand transpiration using allometric relationships between stem diameter and sapwood area for *Cryptomeria japonica* and *Chamaecyparis obtusa*. *For. Ecol. Manag.* **2005**, *206*, 191–195. [[CrossRef](#)]
65. Tie, Q.; Hu, H.C.; Tian, F.Q.; Guan, H.D.; Lin, H. Environmental and physiological controls on sap flow in a subhumid mountainous catchment in North China. *Agric. For. Meteorol.* **2017**, *240–241*, 46–57. [[CrossRef](#)]
66. Ford, C.R.; Hubbard, R.M.; Vose, J.M. Quantifying structural and physiological controls on variation in canopy transpiration among planted pine and hardwood species in the southern Appalachians. *Ecohydrology* **2011**, *4*, 183–195. [[CrossRef](#)]
67. Urban, J.; Rubtsov, A.V.; Urban, A.V.; Shashkin, A.V.; Benkova, V.E. Canopy transpiration of a *Larix sibirica* and *Pinus sylvestris* forest in Central Siberia. *Agric. For. Meteorol.* **2019**, *271*, 64–72. [[CrossRef](#)]
68. Brutsaert, W. An advection-aridity approach to estimate actual regional evapotranspiration. *Water Resour. Res.* **1979**, *15*, 443–450. [[CrossRef](#)]
69. Oren, S.; Katul, G.G.; Pataki, D.E.; Ewers, B.E.; Phillips, N.; Schafer, K.V.R. Survey and synthesis of intra- and interspecific variation in stomatal sensitivity to vapour pressure deficit. *Plant Cell Environ.* **1999**, *22*, 1515–1526. [[CrossRef](#)]
70. Ewers, B.E.; Oren, R.; Johnsen, K.H.; Landsberg, J.J. Estimating maximum mean canopy stomatal conductance for use in models. *Can. J. For. Res.* **2001**, *31*, 198–207. [[CrossRef](#)]
71. Ewers, B.E.; Gower, S.T.; Bond-lamberty, B.; Wang, C.K. Effects of stand age and tree species on canopy transpiration and average stomatal conductance of boreal forests. *Plant Cell Environ.* **2005**, *28*, 660–678. [[CrossRef](#)]
72. Oishi, A.C.; Hawthorne, D.A.; Oren, R. Baseline: An open-source, interactive tool for processing sap flux data from thermal dissipation probes. *SoftwareX* **2016**, *5*, 139–146. [[CrossRef](#)]
73. Schäfer, K.V.R.; Oren, R.; Tenhunen, J.D. The effect of tree height on crown level stomatal conductance. *Plant Cell Environ.* **2000**, *23*, 365–375. [[CrossRef](#)]
74. Wang, G.; Chen, Z.; Shen, Y.; Yang, X. Thinning promoted the rejuvenation and highly efficient use of soil water for degraded *Caragana korshinskii* plantation in semiarid loessal regions. *Land. Degrad. Dev.* **2022**, *34*, 992–1003. [[CrossRef](#)]
75. Tsamir, M.; Gottlieb, S.; Preisler, Y.; Rotenberg, E.; Tatarinov, F.; Yakir, D.; Tague, C.; Klein, T. Stand density effects on carbon and water fluxes in a semi-arid forest, from leaf to stand-scale. *For. Ecol. Manag.* **2019**, *453*, 117573. [[CrossRef](#)]
76. Miller, S.D.; Goulden, M.L.; Huttyra, L.R.; Keller, M.; Saleska, S.R.; Wofsy, S.C.; Figueira, A.M.S.; da Rocha, H.R.; de Camargo, P.B. Reduced impact logging minimally alters tropical rainforest carbon and energy exchange. *Proc. Natl. Acad. Sci. USA* **2011**, *108*, 19431–19435. [[CrossRef](#)]
77. Sinacore, K.; Breton, C.; Asbjornsen, H.; Hernandez-Santana, V.; Hall, J.S. Drought Effects on *Tectona grandis* Water Regulation Are Mediated by Thinning, but the Effects of Thinning Are Temporary. *Front. For. Glob. Chang.* **2019**, *2*, 82. [[CrossRef](#)]
78. Lagergren, F.; Lankreijer, H.; Kucera, J.; Cienciala, E.; Molder, M.; Lindroth, A. Thinning effects on pine-spruce forest transpiration in central Sweden. *For. Ecol. Manag.* **2008**, *255*, 2312–2323. [[CrossRef](#)]
79. Simonin, K.; Kolb, T.E.; Montes-Helu, M.; Koch, G.W. The influence of thinning on components of stand water balance in a ponderosa pine forest stand during and after extreme drought. *Agric. For. Meteorol.* **2007**, *143*, 266–276. [[CrossRef](#)]
80. Li, R.; Han, J.; Guan, X.; Chi, Y.; Zhang, W.; Chen, L.; Wang, Q.; Xu, M.; Yang, Q.; Wang, S. Crown pruning and understory removal did not change the tree growth rate in a Chinese fir (*Cunninghamia lanceolata*) plantation. *For. Ecol. Manag.* **2020**, *464*, 118056. [[CrossRef](#)]
81. Novick, K.A.; Ficklin, D.L.; Stoy, P.C.; Williams, C.A.; Bohrer, G.; Oishi, A.C.; Papuga, S.; Blanken, P.D.; Noormets, A.; Sulman, B.N.; et al. The increasing importance of atmospheric demand for ecosystem water and carbon fluxes. *Nat. Clim. Chang.* **2016**, *6*, 1023–1027. [[CrossRef](#)]

82. Raupach, M. Vegetation–atmosphere interaction and surface conductance at leaf, canopy and regional scales. *Agric. For. Meteorol.* **1995**, *1923*, 151–179. [[CrossRef](#)]
83. Kelliher, F.; Leuning, R.; Raupach, M.R.; Schulze, E.D. Maximum conductances for evaporation from global vegetation types. *Agric. For. Meteorol.* **1995**, *73*, 1–16. [[CrossRef](#)]
84. Yoshifuji, N.; Kumagai, T.O.; Ichie, T.; Kume, T.; Tateishi, M.; Inoue, Y.; Yoneyama, A.; Nakashizuka, T. Limited stomatal regulation of the largest-size class of *Dryobalanops aromatica* in a Bornean tropical rainforest in response to artificial soil moisture reduction. *J. Plant Res.* **2020**, *133*, 175–191. [[CrossRef](#)]
85. Igarashi, Y.; Kumagai, T.; Yoshifuji, N.; Sato, T.; Tanaka, N.; Tanaka, K.; Suzuki, M.; Tantasirin, C. Environmental control of canopy stomatal conductance in a tropical deciduous forest in northern Thailand. *Agric. For. Meteorol.* **2015**, *202*, 1–10. [[CrossRef](#)]
86. Teklehaimanot, Z.; Jarvis, P.G.; Ledger, D.C. Rainfall interception and boundary layer conductance in relation to tree spacing. *J. Hydrol.* **1991**, *123*, 261–278. [[CrossRef](#)]
87. Domec, J.C.; Johnson, D.M. Does homeostasis or disturbance of homeostasis in minimum leaf water potential explain the isohydric versus anisohydric behavior of *Vitis vinifera* L. cultivars? *Tree Physiol.* **2012**, *32*, 245–248. [[CrossRef](#)] [[PubMed](#)]
88. Fischer, M.; Trnka, M.; Kučera, J.; Fajman, M.; Žalud, Z. Biomass productivity and water use relation in short rotation poplar coppice (*Populus nigra* x *P. maximowiczii*) in the conditions of Czech Moravian Highlands. *Acta Univ. Agric. Silv. Mendel. Brun.* **2014**, *59*, 141–152. [[CrossRef](#)]
89. Orság, M.; Trnka, M. Transpiration and biomass increment in short rotation poplar coppice. In Proceedings of the International PhD Students Conference “MendelNet”, Brno, Czech Republic, 23 November 2011; pp. 688–693.
90. Li, X.; Aini Farooqi, T.J.; Jiang, C.; Liu, S.; Sun, O.J. Spatiotemporal variations in productivity and water use efficiency across a temperate forest landscape of Northeast China. *For. Ecosyst.* **2019**, *6*, 22. [[CrossRef](#)]
91. He, Q.; Yan, M.; Miyazawa, Y.; Chen, Q.; Cheng, R.; Otsuki, K.; Yamanaka, N.; Du, S. Sap flow changes and climatic responses over multiple-year treatment of rainfall exclusion in a sub-humid black locust plantation. *For. Ecol. Manag.* **2020**, *457*, 117730. [[CrossRef](#)]
92. Xue, P.; Miao, N.; Yue, X.; Tao, Q.; Zhang, Y.; Peng, Z.; Mao, K. Excessive Rainfall in Growing Season May Cause Tree Growth Decline in Minjiang Fir on the Eastern Tibetan Plateau. 2022. Available online: <https://ssrn.com/abstract=4145839> (accessed on 24 June 2022).
93. Rahman, M.; Islam, M.; Bräuning, A. Tree radial growth is projected to decline in South Asian moist forest trees under climate change. *Glob. Chang. Biol.* **2018**, *170*, 106–119. [[CrossRef](#)]
94. Huang, K.; Xu, C.; Qian, Z.; Zhang, K.; Tang, L. Effects of Pruning on Vegetation Growth and Soil Properties in Poplar Plantations. *Forests* **2023**, *14*, 501. [[CrossRef](#)]

**Disclaimer/Publisher’s Note:** The statements, opinions and data contained in all publications are solely those of the individual author(s) and contributor(s) and not of MDPI and/or the editor(s). MDPI and/or the editor(s) disclaim responsibility for any injury to people or property resulting from any ideas, methods, instructions or products referred to in the content.